

Uncertainty-aware Sensitivity Analysis Using Rényi Divergences

Topi Paananen¹
topi.paananen@aalto.fi

Michael Riis Andersen²
miri@dtu.dk

Aki Vehtari¹
aki.vehtari@aalto.fi

¹Helsinki Institute for Information Technology, HIIT

¹Aalto University, Department of Computer Science

²Department of Applied Mathematics and Computer Science, Technical University of Denmark

Abstract

For nonlinear supervised learning models, assessing the importance of predictor variables or their interactions is not straightforward because it can vary in the domain of the variables. Importance can be assessed locally with sensitivity analysis using general methods that rely on the model’s predictions or their derivatives. In this work, we extend derivative based sensitivity analysis to a Bayesian setting by differentiating the Rényi divergence of a model’s predictive distribution. By utilising the predictive distribution instead of a point prediction, the model uncertainty is taken into account in a principled way. Our empirical results on simulated and real data sets demonstrate accurate and reliable identification of important variables and interaction effects compared to alternative methods.

1 Introduction

Identifying important features and interactions from complex data sets and models remains a topic of active research. This is a fundamental problem with important applications in many scientific disciplines. Often the goal is to improve understanding of the model, but the identified features and interactions can also be used to build a simpler or more interpretable surrogate model.

For models that can capture nonlinear effects and interactions, the typical approach is to assess the contributions of individual predictors or interactions on the model’s prediction at an individual observation. One approach is sensitivity analysis, which evaluates the change in predictions to small perturbations in the predictor values. For example, the partial derivative of the

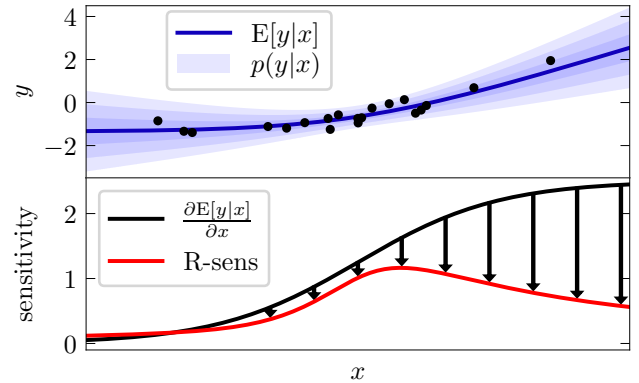


Figure 1: Top: Example of data and a probabilistic model with a Gaussian predictive distribution $p(y|x)$. The different shades of blue represent 1, 2, and 3 standard deviations of the predictive distribution. Bottom: The derivative of $E[y|x]$ with respect to x (black) represents the naive sensitivity of the model’s predictions to changes in x . The R-sens method proposed in this work (red) represents uncertainty-aware sensitivity as given by differentiating a Rényi divergence of predictive distributions, which adjusts the sensitivity according to uncertainty about y .

model’s prediction with respect to the predictors can be a measure of importance (Cacuci, 2003; Oakley and O’Hagan, 2004; Cacuci et al., 2005; Guyon and Elisseeff, 2003). Since the derivative can vary from positive to negative in the domain of the predictors, most approaches use absolute or squared derivatives averaged from the observations (Ruck et al., 1990; Dorizzi, 1996; Czernichow, 1996; Refenes and Zapanis, 1999; Leray and Gallinari, 1999; Sundararajan et al., 2017; Cui et al., 2020). A similar approach is popular in image classification, where derivatives with respect to each pixel are called saliency maps (Simonyan et al., 2013; Zeiler and Fergus, 2014; Guidotti et al., 2018). The average predictive comparison of Gelman and Pardoe (2007) uses the difference quotient of two predictions without

taking the limit. By extending to cross-derivatives with respect to two predictors, one can also measure the interaction effect of predictors (Friedman et al., 2008; Cui et al., 2020). A closely related approach for sensitivity analysis is to directly estimate the contribution of predictor main effects or interactions to the variance of the target variable (IM, 1993; Homma and Saltelli, 1996; Oakley and O’Hagan, 2004; Saltelli, 2002).

Recently, approaches that evaluate the differences of predictions in permuted training observations have gained popularity in machine learning. For example, Fisher et al. (2019) permute the observations of a single predictor, and examine the loss in predictive ability compared to the original data. Shapley values use permutations to assess the average marginal contribution of a predictor to a specific observation (Shapley, 1953; Štrumbelj and Kononenko, 2014). Lundberg et al. (2018) extended this approach to evaluate second-order interactions based on the Shapley interaction index (Fujimoto et al., 2006). Friedman et al. (2008) and Greenwell et al. (2018) use permutations and partial dependence functions (Friedman, 2001) to construct statistics that measure the strength of pairwise interactions. The individual conditional expectation plots of Goldstein et al. (2015) can also be used to identify interactions, but they rely on visualisation only.

The contributions of this work are summarised as follows. First, we present a novel method that generalises derivative and Hessian based sensitivity analysis to a Bayesian setting for models with a parametric predictive distribution or its approximation. Instead of using the first or second derivatives of the mean prediction of the model, we instead differentiate the Rényi divergence from one predictive distribution to another, which takes into account the epistemic uncertainty of the predictions. Figure 1 gives an illustration of this method. Second, we show that our method is an analytical generalisation and extension of a previous finite difference method (Paananen et al., 2019). Third, we show empirically that our proposed method can improve the accuracy of sensitivity analysis in situations where the used model has significant predictive uncertainty. Code for our method and simulations is available at <https://github.com/topipa/rsens-paper>.

2 Uncertainty-Aware Sensitivity

Consider a supervised learning model trained on data (\mathbf{X}, \mathbf{y}) , where $\mathbf{X} \in \mathbb{R}^{N \times D}$ is the design matrix and $\mathbf{y} \in \mathbb{R}^N$ is the vector of target observations. Let us denote the prediction function of the model for the target variable y as $f(\mathbf{x}^*)$. Derivative based sensitivity analysis can be used to assess the local sensitivity of f to the different predictors $(x_d)_{d=1}^D$. The sensitivity can

be quantified by the partial derivative

$$\frac{\partial f(\mathbf{x}^*)}{\partial x_d^*}.$$

Absolute values of local derivatives can be aggregated over the empirical distribution of \mathbf{x} to obtain a global importance estimate for x_d , the expected absolute derivative (EAD)

$$\text{EAD}(x_d) = \mathbb{E}_{p(\mathbf{x})} \left[\left| \frac{\partial f(\mathbf{x})}{\partial x_d} \right| \right].$$

Similarly, absolute values of the elements of the Hessian matrix of f , that is, the second derivatives with respect to x_d and x_e , quantify the sensitivity to the joint interaction effect of x_d and x_e .

In this section, we present our proposed R-sens method that extends derivative and Hessian based sensitivity analysis methods to a Bayesian setting where the evaluated model not only has a function for point predictions, but a *predictive distribution* $p(y^*)$. For now, we only consider predictive distributions that have some parametric form, which can be obtained exactly in closed form or it can be an approximation. Because the predictive distribution is obtained by integrating over posterior uncertainty for the model parameters, it is important to utilise this uncertainty in sensitivity analysis as well.

To formulate a derivative based sensitivity measure for a model with a predictive distribution, we need a suitable functional of the predictive distribution, which to differentiate. We choose a family of statistical divergences called Rényi divergences due to their convenient properties, which we discuss later in this section. Rényi divergence of order α is defined for two probability mass functions $P = (p_1, \dots, p_n)$ and $Q = (q_1, \dots, q_n)$ as

$$\mathcal{D}_\alpha[P||Q] = \frac{1}{\alpha - 1} \log \left(\sum_{i=1}^n \frac{p_i^\alpha}{q_i^{\alpha-1}} \right)$$

when $0 < \alpha < 1$ or $1 < \alpha < \infty$ (Rényi et al., 1961; Van Erven and Harremoës, 2014). The definition generalises to continuous spaces by replacing the probabilities by densities and the sum by an integral. The divergences for values $\alpha = 0, 1$, and ∞ are obtained as limits. The most well-known Rényi divergence is the Kullback-Leibler divergence which is obtained in the limit $\alpha \rightarrow 1$ (Kullback and Leibler, 1951).

Let us consider a model with a predictive distribution parametrised by a vector $\boldsymbol{\lambda}^* = (\lambda_1^*, \dots, \lambda_M^*)$, which possibly depends on \mathbf{x}^* . Let us denote the predictive distribution for y conditional on predictor values \mathbf{x}^* as

$$p(y^*) \equiv p(y^* | \boldsymbol{\lambda}^*(\mathbf{x}^*)).$$

Keeping \mathbf{x}^* fixed, we denote the Rényi divergence of order α between two predictive distributions as a function of \mathbf{x}^{**} as

$$\mathcal{D}_\alpha^p[\mathbf{x}^{**}] \equiv \mathcal{D}_\alpha[p(y^*|\boldsymbol{\lambda}^*(\mathbf{x}^*))||p(y^*|\boldsymbol{\lambda}^*(\mathbf{x}^{**}))].$$

We formalise the sensitivity of the predictive distribution to a change in a single predictor variable by differentiating the Rényi divergence in the limit when the distributions coincide, that is when $\mathbf{x}^{**} = \mathbf{x}^*$. However, because Rényi divergences obtain their minimum value when the two distributions coincide, the first derivative at this point is always zero. Hence, we formulate the uncertainty-aware sensitivity measure with respect to the predictor x_d using the second derivative

$$\frac{\partial^2 \mathcal{D}_\alpha^p[\mathbf{x}^{**}]}{(\partial x_d^{**})^2} \Big|_{\mathbf{x}^{**}=\mathbf{x}^*} = \left(\frac{\partial \boldsymbol{\lambda}^*(\mathbf{x}^*)}{\partial x_d^*} \right)^T \mathbf{H}_{\boldsymbol{\lambda}^*(\mathbf{x}^{**})}(\mathcal{D}_\alpha^p[\mathbf{x}^{**}]) \left(\frac{\partial \boldsymbol{\lambda}^*(\mathbf{x}^{**})}{\partial x_d^{**}} \right) \Big|_{\mathbf{x}^{**}=\mathbf{x}^*}, \quad (1)$$

where $\mathbf{H}_{\boldsymbol{\lambda}^*(\mathbf{x}^{**})}$ is the Hessian matrix of the Rényi divergence with second order derivatives with respect to $\boldsymbol{\lambda}^*(\mathbf{x}^{**})$.

The sensitivity measure in equation (1) has two kinds of partial derivatives: (i) second order derivatives of the Rényi divergence with respect to the parameters $\boldsymbol{\lambda}^*$ of the predictive distribution, and (ii) first order derivatives of the parameters $\boldsymbol{\lambda}^*$ with respect to the predictor x_d^* . These are obtained as follows:

- (i) For sufficiently regular parametrisations, the second order Taylor approximation of the Kullback-Leibler divergence ($\alpha = 1$) gives an approximate equivalence between the Hessian of the divergence and the Fisher information matrix of $p(y^*)$ in the limit $\mathbf{x}^{**} - \mathbf{x}^* \rightarrow 0$ (Kullback, 1959; Van Erven and Harremos, 2014). Haussler et al. (1997) state that this generalises to any Rényi divergence with $0 < \alpha < \infty$, leading to the relation

$$\mathbf{H}_{\boldsymbol{\lambda}^*(\mathbf{x}^{**})}(\mathcal{D}_\alpha^p[\mathbf{x}^{**}]) \Big|_{\mathbf{x}^{**}=\mathbf{x}^*} \approx \alpha \mathcal{I}(\boldsymbol{\lambda}^*(\mathbf{x}^*)), \quad (2)$$

where $\mathcal{I}(\boldsymbol{\lambda}^*(\mathbf{x}^*))$ is the Fisher information matrix of the distribution $p(y^*|\boldsymbol{\lambda}^*(\mathbf{x}^*))$.

- (ii) The partial derivative of the parameter λ_k^* with respect to predictor variable x_d^* depends on the model where the predictive distribution is from.

We define R-sens, an uncertainty-aware sensitivity measure for predictor x_d at \mathbf{x}^* as

$$\text{R-sens}(\mathbf{x}^*, x_d, \alpha) \equiv \sqrt{\alpha \left(\frac{\partial \boldsymbol{\lambda}^*}{\partial x_d^*} \right)^T \mathcal{I}(\boldsymbol{\lambda}^*(\mathbf{x}^*)) \left(\frac{\partial \boldsymbol{\lambda}^*}{\partial x_d^*} \right)}. \quad (3)$$

When using R-sens in sensitivity analysis for comparing predictors, the value of α does not matter in practice and we use the value $\alpha = 1$.

In a similar fashion as above, we generalise the Hessian based sensitivity to a Bayesian predictive distribution by differentiating the Rényi divergence four times, i.e. twice with respect to two predictors. The full fourth derivative contains cross-derivative terms, which we drop for two reasons. First, based on our experiments we concluded that the simplified formula we use is better at identifying interactions, meaning that the dropped terms do not contain useful information about the interaction effect between x_d and x_e . Second, the simplified formula is similar to the R-sens measure and is thus more easily interpretable and computationally cheaper. We define R-sens₂, the uncertainty-aware sensitivity measure for the interaction effect between variables x_d and x_e as

$$\begin{aligned} & \text{R-sens}_2(\mathbf{x}^*, (x_d, x_e), \alpha) \\ & \equiv \sqrt{\alpha \left(\frac{\partial^2 \boldsymbol{\lambda}^*}{\partial x_d^* \partial x_e^*} \right)^T \mathcal{I}(\boldsymbol{\lambda}^*(\mathbf{x}^*)) \left(\frac{\partial^2 \boldsymbol{\lambda}^*}{\partial x_d^* \partial x_e^*} \right)}. \end{aligned} \quad (4)$$

In the supplementary material, we show the full equation and an illustration of the benefit of equation (4) compared to the full fourth derivative.

2.1 Location-Scale Family

For distributions in the location-scale family ($p(y|\lambda_1, \lambda_2) = g((y - \lambda_1)/\lambda_2)/\lambda_2$), the Fisher information of the location parameter is independent of the location parameter (Shao, 2006, Ex. 20). This has two implications. First, if the predictive distribution is in the location-scale family, the R-sens and R-sens₂ measures are direct extensions to the absolute derivative or absolute Hessian of the mean prediction. The extension is twofold, as they introduce the derivative of the scale parameter and possible auxiliary parameters, and also multiplication with the Fisher information matrix. The uncertainty-aware measures can be also viewed as the Mahalanobis norm of the differentiated parameters of the predictive distribution instead of a simple Euclidean norm. Second, for a sufficiently regular model, where the posterior uncertainty vanishes in the asymptotic regime due to the Bernstein-von Mises theorem (Walker, 1969) such that the predictive distribution converges to a limiting distribution in the location-scale family, R-sens tends to the absolute derivative of the mean prediction. Here, we have to assume that the Fisher information exists and converges to the Fisher information of the limiting distribution.

2.2 Illustrative Example

To illustrate the effects of the different components in equation (3), we analyse a Bayesian linear regression model as an example. We use the standard Gaussian likelihood with noise variance σ^2 and denote the regression coefficients as β . Using an improper uniform prior on $(\beta, \log \sigma)$, integrating over the uncertainty about all the parameters makes the posterior predictive distribution at any point \mathbf{x}^* (treated as a row vector)

$$\begin{aligned} p(y^*|\mathbf{X}, \mathbf{y}) &= \text{Student-}t(\mathbb{E}[y^*], \text{Var}[y^*], \nu), \text{ where} \\ \mathbb{E}[y^*] &= \mathbf{x}^* \hat{\beta}, \\ \text{Var}[y^*] &= s^2(1 + \mathbf{x}^*(\mathbf{X}^T \mathbf{X})^{-1} \mathbf{x}^{*T}), \\ \nu &= N - D, \\ \hat{\beta} &= (\mathbf{X}^T \mathbf{X})^{-1} \mathbf{X}^T \mathbf{y}, \\ s^2 &= \frac{(\mathbf{y} - \mathbf{X} \hat{\beta})^T (\mathbf{y} - \mathbf{X} \hat{\beta})}{N - D}. \end{aligned}$$

Here, ν represents the degrees of freedom, N and D are the number of observations and predictor variables, respectively, and $\hat{\beta}$ are the maximum likelihood estimates of the regression coefficients. The derivative of ν with respect to x_d^* is zero, and the derivatives of the other two parameters of $p(y^*|\mathbf{X}, \mathbf{y})$ are

$$\begin{aligned} \frac{\partial \mathbb{E}[y^*]}{\partial x_d^*} &= \hat{\beta}_d, \\ \frac{\partial \text{Var}[y^*]}{\partial x_d^*} &= 2s^2[(\mathbf{X}^T \mathbf{X})^{-1} \mathbf{x}^{*T}]_d \equiv 2s^2 V_d. \end{aligned}$$

Multiplying these with the Fisher information matrix of the Student- t predictive distribution, the R-sens sensitivity measure for the predictor x_d from equation (3) evaluates to

$$\text{R-sens}(\mathbf{x}^*, x_d, \alpha = 1) = \sqrt{\frac{(\nu + 1) \hat{\beta}_d^2 + \frac{+2\nu s^4 V_d^2}{\text{Var}[y^*]}}{(\nu + 3) \text{Var}[y^*]}}. \quad (5)$$

The two summands have the following interpretations: In the absence of the second term, the measure would be proportional to $|\hat{\beta}_d|$ divided by the standard deviation of the predictive distribution. The first term thus measures the absolute derivative of the mean prediction, but predictions with high uncertainty are given less weight. Also the second term in equation (5) quantifies the amount of uncertainty in the predictive distribution, but in a different way. Even if $\hat{\beta}_d$ would be exactly zero, the second summand is nonzero as long as there is uncertainty about the model parameters that causes the predictive uncertainty to vary with respect to \mathbf{x}^* . There are thus two separate mechanisms that include epistemic uncertainty in the sensitivity analysis (O'Hagan, 2004; Kendall and Gal, 2017). As

N (and hence also ν) approaches infinity and the posterior uncertainty vanishes, the R-sens measures for both variables approach a constant proportional to $|\hat{\beta}_d|$.

To visualise the effects of the two terms in equation (5), we simulated 10 observations from a linear model with two predictor variables x_1 and x_2 whose true regression coefficients are $\beta_1 = 1$ and $\beta_2 = 0$. The predictor variables are independent and normally distributed with zero mean and standard deviation one, and the simulated noise standard deviation is $\sigma_{\text{true}} = 0.5$. The R-sens sensitivities for both variables are shown in the bottom part of Figure 2. The red color depicts the predictive distribution $p(y|x_1, x_2 = 0)$ (top) and R-sens for x_1 (bottom). The R-sens value is dominated by the contribution from the first summand in equation (5), where the Fisher information weighs down the sensitivity at the edges of the data because of the larger uncertainty. The blue color shows the predictive distribution $p(y|x_2, x_1 = 0)$ and R-sens for x_2 . Now the first summand in equation (5) is almost zero because $\hat{\beta}_2$ is so small. In this case, the second term dominates because there is still a significant amount of epistemic uncertainty in the model. Comparing R-sens for x_1 and x_2 illustrates the two different ways that R-sens takes uncertainty into account.

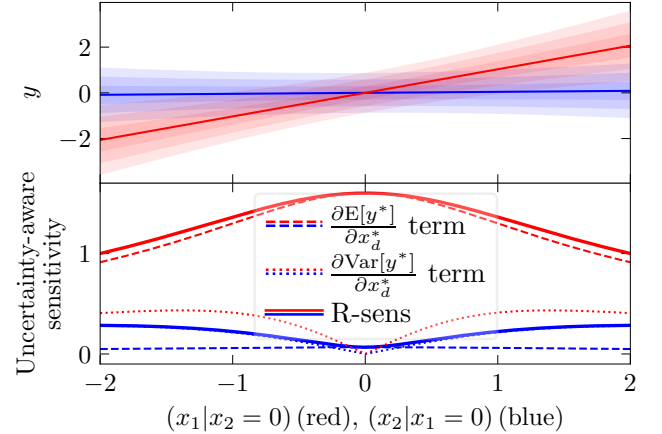


Figure 2: Top: Predictive distributions $p(y|x_1, x_2 = 0)$ (red) and $p(y|x_2, x_1 = 0)$ (blue) for the linear regression model in Section 2.2. Bottom: R-sens uncertainty-aware sensitivity measure for x_1 (red) and x_2 (blue). The dashed and dotted lines show the contributions of the two summands in equation (5).

Note that R-sens is model-agnostic in the sense that it does not take into account the fact that the prediction function is constrained to be linear in the example above. In addition, the different terms in equation (3) may not have such clear interpretations for other likelihoods or models. For example, in a binary classification task, the posterior predictive distribution can be considered a Bernoulli distribution which has only a single

parameter. Nevertheless, the principle of taking into account the uncertainty through the predictive distribution still holds.

2.3 Applicability

The requirements for using the proposed R-sens and R-sens₂ methods are that we must have an analytical representation of the predictive distribution conditioned on the predictor variables, and that the derivatives of its parameters with respect to the predictors must be available. This somewhat restricts their applicability, but computational tools such as automatic differentiation make practical implementation easier (Baydin et al., 2018). There are no restrictions to the support of the predictive distribution, and the methods are thus applicable to many learning tasks. However, because the methods adjust sensitivity based on the model uncertainty, the results may be misleading if the model lacks proper uncertainty quantification. We thus recommend using the methods for probabilistic models where the uncertainty is properly taken into consideration. In practice, the methods are most useful when the number of observations is relatively small and there is a lot of uncertainty about the parameters of the model.

Because the proposed methods measure the importance of predictor variables locally, they are most useful for nonlinear and complex models. For example, they can be useful for sensitivity analysis with Gaussian process models, which can represent flexible nonlinear functions with interactions, but still have good uncertainty quantification (O’Hagan, 1978; MacKay, 1998; Neal, 1998; Rasmussen and Williams, 2006). Moreover, the predictive distribution is available in a parametric form, although for certain likelihoods some approximations are required. In the supplementary material we show the derivatives required for the R-sens and R-sens₂ methods for Gaussian processes and commonly used likelihoods.

The added computational expense of the R-sens and R-sens₂ methods compared to just differentiating the mean prediction depends on the used model. For many models, the cost is not significant compared to the cost of inference.

2.4 Finite Difference Approximation

Paananen et al. (2019) propose a sensitivity analysis method abbreviated KL, which is a finite difference like method that evaluates the Kullback-Leibler divergence of predictive distributions when the predictor variables are perturbed. If we set $\alpha = 1$ (where Rényi divergence equals the Kullback-Leibler divergence), we show that the KL method is approximately equivalent to the

second order Taylor approximation of R-sens

$$\text{R-sens}(\mathbf{x}^*, x_d, \alpha = 1) \approx \frac{\sqrt{2\mathcal{D}_1[p(y^*|\boldsymbol{\lambda}^*(\mathbf{x}^*))||p(y^*|\boldsymbol{\lambda}^*(\mathbf{x}^{**}))]}}{|x_d^{**} - x_d^*|}.$$

Here, \mathbf{x}^{**} is equivalent to \mathbf{x}^* with predictor x_d perturbed, and \mathcal{D}_1 denotes the Kullback-Leibler divergence. Due to space constraints, we show the full derivation in the supplementary material. The benefit of the finite difference approximation is generality as it requires only an analytical representation of the predictive distribution but not the derivatives of its parameters with respect to the predictors. However, using R-sens avoids numerical errors related to finite difference and is easier because the selection of the perturbation size is avoided. For an appropriately chosen perturbation, the two equations produce practically identical results up to a small numerical error.

Our proposed R-sens₂ measure is not directly approximable with finite differences in the same way as R-sens. This is because it would require second-order finite differences, but the first-order finite difference using Kullback-Leibler divergence already reduces the predictive distribution into a single number. Riihimäki et al. (2010) perturb two predictor variables at a time with a unit length perturbation and measure the change in predictions by Kullback-Leibler divergence. For an infinitesimal perturbation this would be equivalent to a directional derivative instead of the cross-derivative in the R-sens₂ method that is required to properly assess interaction effects.

3 Experiments

In this section, we demonstrate the practical utility of the methods discussed in Section 2 for identifying important predictor variables and interactions in nonlinear models. First, we evaluate different variable importance methods on simulated data using a hypothetical predictive function. This way we can control the quality of the model fit and limit the comparison strictly to the variable importance methods. Second, we will use Gaussian process models to evaluate ranking of main effects and interactions on both simulated and real data.

We compare the R-sens and R-sens₂ measures to several alternative variable importance methods: 1) Expected absolute derivative (EAD) or expected absolute Hessian (EAH), which correspond to R-sens and R-sens₂ without predictive uncertainty, 2) Absolute expected derivative (AED) or absolute expected Hessian (AEH) that take the expectation over \mathbf{x} inside the absolute value (Cui et al., 2020), 3) Average predictive comparison (APC) (Gelman and Pardoe, 2007), 4) Shapley

values (Shapley, 1953; Štrumbelj and Kononenko, 2014; Lundberg et al., 2018), 5) Partial dependence based importance (PD) (Greenwell et al., 2018), 6) Permutation feature importance (PFI) (Fisher et al., 2019), 7) Variance of the predictive mean (VAR) (Paananen et al., 2019), and 8) H-statistic (Friedman et al., 2008). We omit comparison to the KL method of Paananen et al. (2019) because it is equivalent to R-sens up to numerical accuracy. We still show the results of their VAR method, which has no direct connection to R-sens. We have used the methods such that their computational cost is approximately equivalent. In the supplementary material, we detail the practical computational cost of the compared methods.

For assessing the global importance of predictor variables or pairs of variables, we aggregate the local R-sens and R-sens₂ sensitivity measures over the empirical distribution of the predictors. Using the global measures, we can rank the predictor variables or pairwise interactions.

3.1 Simulated Individual Effects

In the first experiment we compare different methods for ranking individual predictors based on their importance. We simulate 200 observations from 10 predictors, and construct the target variable y as a sum of 10 effects with added Gaussian noise

$$x_i \sim p_{x_i}(x_i), \quad i = 1, \dots, 10,$$

$$y = f_{\text{true}}(\mathbf{x}) = \sum_{i=1}^{10} A_i f_{\text{true},i}(x_i) + \varepsilon.$$

The shape of each effect $f_{\text{true},i}(x_i)$ is the same for all i , but they have different strengths varying from $A_1 = 1$ to $A_{10} = 10$. We consider 6 different experiments with different function shapes. By considering only a single effect shape for each experiment, we can unambiguously define the true importance of each predictor. We also repeat the experiment with 4 different distributions for the predictors.

When evaluating the ranking methods, we first use the true data generating function $f_{\text{true}}(\mathbf{x})$ as the mean prediction of the model. To simulate the uncertainty of the prediction model, we set the predictive distribution as Gaussian whose variance increases quadratically as distance from the mean of the data increases. Using the true data generating function allows us to strictly compare the ranking methods without being obscured by a non-optimal model fit. Because all of the compared methods use the mean prediction for ranking the predictors, using the true data generating function does not favour any single method over the others.

To consider the effect of taking uncertainty into account

in the ranking, we also consider an imperfect version of the ground-truth model, where each term $A_i f_{\text{true},i}(x_i)$ is multiplied with a term $(|A_{\text{bias},i}| |x_i|^3 + 1)$ where $A_{\text{bias},i}$ is drawn from a normal distribution with mean 0 and standard deviation 0.02. This simulates a situation where the model is correct where the uncertainty is small, but is biased at the edges of the data where the uncertainty is larger.

In Table 1 we show the results of different ranking methods for 6 different functions $f_{\text{true}}(\mathbf{x})$. Here, the distributions p_{x_i} of the predictors are independent Student- t_3 distributions. In the supplementary material, we show the results of the experiment with three alternative distributions p_{x_i} . The results are generated from 500 independent repetitions. In each repetition, the 10 predictors are ranked in importance from 1 to 10. For each data realisation, we compute the average error in the ranks across the predictors with respect to the true ranking, and compare that error to the ranking error of R-sens. A negative number thus means that the error is on average smaller than for R-sens. Table 1 reports the mean and 95% uncertainty intervals of the comparative ranking errors across the 500 independent data realisations.



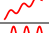
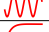
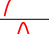
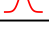


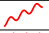
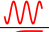
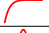

The top section of Table 1 shows the ranking errors when using the ground-truth predictions function. R-sens and EAD are almost equivalent in many cases, but R-sens is significantly better for functions that have a large derivative in the tails of the data (x^3 and $x \exp(-x)$). Both R-sens and EAD outperform the other methods in most cases. AED does well for function that are monotonic, but it fails badly for non-monotonic functions. This is expected because the derivative of these functions varies from positive to negative.

In the bottom section of Table 1 when the model's predictions are imperfect, the difference in the ranking errors of R-sens and EAD is significantly larger in favour of R-sens. R-sens is also consistently better than the alternative methods with just a few exceptions. This shows that the uncertainty-aware sensitivity can be more reliable when there is a significant amount of uncertainty. In the supplementary material, we repeat the experiment with three alternative distributions p_{x_i} , including independent and correlated normal distributions. These results have similar conclusions: R-sens is mostly similar to EAD, but better in specific situations.

3.2 Simulated Individual and Pairwise Effects

In the second experiment, we study how accurately different methods evaluate interactions when the model has both main effects and interaction effects. We sim-

Table 1: Average relative errors in rankings compared to R-sens and 95% uncertainty intervals from 500 data realisations in the simulated example of Section 3.1. A negative value indicates better ranking than R-sens.

Ground-truth models									
Function $f_{\text{true},i}(x)$	R-sens	EAD	AED	APC	SHAP	PD	PFI	VAR	
 x	0	0.0 ± 0.0	0.0 ± 0.0	0.0 ± 0.0	0.0 ± 0.0	2.3 ± 0.2	1.1 ± 0.1	3.6 ± 0.2	3.9 ± 0.2
 x^3	0	2.0 ± 0.2	2.0 ± 0.2	9.5 ± 0.5	10.0 ± 0.4	1.2 ± 0.3	15.8 ± 0.5	5.7 ± 0.3	
 $x + \cos(3x)$	0	-0.1 ± 0.0	4.0 ± 0.2	5.9 ± 0.3	1.7 ± 0.2	1.8 ± 0.2	2.8 ± 0.2	3.0 ± 0.2	
 $\sin(3x)$	0	0.0 ± 0.0	20.3 ± 0.6	11.5 ± 0.4	0.4 ± 0.1	0.3 ± 0.1	0.4 ± 0.1	8.3 ± 0.5	
 $x \exp(-x)$	0	0.6 ± 0.1	0.6 ± 0.1	0.7 ± 0.3	1.1 ± 0.2	-16.5 ± 0.7	5.6 ± 0.7	-4.6 ± 0.7	
 $\exp(-x^2)$	0	0.0 ± 0.0	20.5 ± 0.6	9.3 ± 0.3	0.3 ± 0.1	-0.1 ± 0.1	0.3 ± 0.1	0.0 ± 0.1	
Imperfect models									
Function $f_{\text{true},i}(x)$	R-sens	EAD	AED	APC	SHAP	PD	PFI	VAR	
 x	0	2.6 ± 0.5	2.7 ± 0.5	10.8 ± 0.7	20.1 ± 0.7	22.4 ± 0.9	21.3 ± 0.7	1.1 ± 0.4	
 x^3	0	1.4 ± 0.5	1.7 ± 0.5	6.7 ± 0.7	9.7 ± 0.8	12.3 ± 0.9	9.7 ± 0.8	-4.4 ± 0.5	
 $x + \cos(3x)$	0	2.6 ± 0.4	6.7 ± 0.5	14.0 ± 0.6	23.4 ± 0.7	25.1 ± 0.9	24.8 ± 0.6	4.0 ± 0.4	
 $\sin(3x)$	0	2.1 ± 0.3	18.9 ± 0.6	10.5 ± 0.5	14.8 ± 0.6	5.3 ± 0.9	20.8 ± 0.7	1.0 ± 0.3	
 $x \exp(-x)$	0	0.2 ± 0.3	0.5 ± 0.3	4.3 ± 0.8	3.9 ± 0.8	5.2 ± 1.0	4.0 ± 0.8	-2.7 ± 0.8	
 $\exp(-x^2)$	0	0.0 ± 0.0	20.6 ± 0.6	9.1 ± 0.3	0.3 ± 0.1	0.0 ± 0.1	0.3 ± 0.1	0.0 ± 0.1	

ulate 12 predictors and 8 main effects with different shapes and strengths, and three equally important pairwise interaction effects which are simply the product of the two predictors, i.e. $x_d x_e$. These are chosen such that the predictors of the first interaction do not have main effects, one of the predictors in the second interaction has a main effect, and both predictors of the third interaction have a main effect. To study how many observations the different methods require to reliably detect the true interactions in the data, we generate data with different numbers of observations ranging from 50 to 300.

In Figure 3, we plot the importance values averaged from 50 simulations for the three interacting variable pairs as well as three variable pairs without an interaction effect. The solid lines represent pairs with a true interaction, and the dotted lines are pairs without an interaction. In the left plot, both variables in the pairs have a main effect. In the middle plot, only one variable in the pairs has a main effect, and in the right plot neither variable has a main effect. For each of the 50 simulations, the interaction importance values are scaled so that the maximum given by each method is one. Thus, the ideal value is 1 for the solid lines and 0 for the dotted lines.

Figure 3 shows that even when increasing the number of observations, the HS method over-emphasizes the variable pair where neither variable has a main effect (right plot), whereas the PD method over-emphasizes the variable pair where both variables have a main effect (left plot). The other methods correctly identify the interactions as equally relevant when increasing the number of observations. For the true interactions (solid

lines), EAH and R-sens₂ are almost indistinguishable, but R-sens₂ gives higher importance to the nonexistent interactions (dotted lines) when there is significant uncertainty because the number of observations is small.

3.3 Benchmark Data Sets

In real data experiments, we focus on assessing the performance of the pairwise interaction method R-sens₂, because the experiments of Paananen et al. (2019) already demonstrate the effectiveness of (the finite difference approximation of) R-sens empirically. We use two publicly available data sets. The first is the Concrete Slump data set where the compressive strength of concrete is predicted based on the amount of different components included (Yeh, 2007). The second is a Bike sharing data set, where the target variable is the hourly number of bike uses from a bicycle rental system (Fanaee-T and Gama, 2014). The Concrete data has 103 observations and 7 predictors. From the Bike sharing data, we picked observations from February across two years, resulting in 1339 observations and 6 predictors. We model the problems using Gaussian process models with an exponentiated quadratic covariance function and either Gaussian (Concrete) or Poisson (Bike) likelihood. With the Poisson likelihood, we use the Laplace approximation for the latent values, and thus the resulting predictive distribution is an approximation but has an analytical solution. The details of the models and the derivatives needed for R-sens₂ are presented in the supplementary material.

To evaluate the plausibility of the interactions identified by the different methods, we compare the out-of-sample

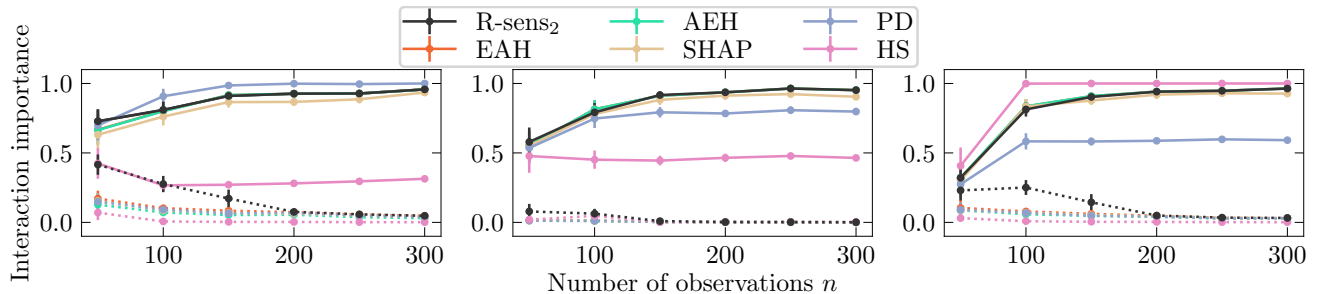


Figure 3: The interaction importance values given to six variable pairs in data sets with different numbers of observations. The solid lines represent pairs with a true interaction, and dotted lines are pairs without an interaction. The left plot depicts two pairs where both variables in the pairs have a main effect. In the middle plot, only one variable in the pairs has a main effect, and in the right plot neither variable has a main effect. In all plots, the ideal values would be 1 and 0 for the solid and dotted lines, respectively. The error bars represent 95% uncertainty intervals for the means from 50 simulated data sets.

predictive performance of models with explicit interaction terms chosen based on interactions identified by each method. We compare the performance of the models using cross-validation with 50 random splits into training and test sets, and log predictive density as the utility function. The number of training observations used is 80 in the Concrete data and 500 in the Bike sharing data. For each training set, the Gaussian process model with full interactions is fitted, and the pairwise interactions are identified with R-sens₂ and 5 other methods. Based on these, models with only 0 to 5 pairwise interaction terms are fitted again, and their predictive performance is evaluated on the test data.

The mean log predictive densities (MLPDs) across different test splits as well as 95% uncertainty intervals of the means are shown in Figure 4. The figure shows that in the Bike sharing data, modelling only the three strongest pairwise interactions increases the out-of-sample predictive performance to the level of the model with all possible interactions. R-sens₂ does equally well compared to EAH, which both identify more important interactions than the competing methods. In the Concrete data set, adding even 5 pairwise interactions does not reach the performance of the model with all interactions. In this data there are no significant differences between the methods, except for HS which is clearly worse than the rest.

We also evaluate the stability of the interaction rankings by computing the variability in the rankings across 100 Bootstrap samples of the data. Table 2 shows the entropy in the rankings of each method across the Bootstrap samples. In both data sets, R-sens₂ and EAH have smaller entropies than the competing methods, meaning that their rankings are more stable.

Table 2: Variability in rankings across different Bootstrap samples of the benchmark data sets.

Data	R-sens ₂	EAH	AEH	PD	HS	SHAP
Concrete	1.86	1.80	1.99	2.04	2.26	1.90
Bike	1.61	1.63	2.28	2.16	2.61	2.58

4 Conclusion

In this work, we presented an uncertainty-aware sensitivity analysis method that is based on differentiating Rényi divergences of predictive distributions. We showed that the method takes model uncertainty into account in a principled way and generalises to different likelihoods. For likelihoods in the location-scale family, the method is a direct extension to the absolute derivative or absolute Hessian of the mean prediction which are non-Bayesian sensitivity measures. Even though the method generalises to different predictive distributions, we recommend using it for models that have well calibrated uncertainty. The proposed method requires an analytical representation of the predictive distribution of the model, which is not available for all models. This could be generalised further, which is a possible direction for future research.

We demonstrated empirically that the method can reliably identify main effects as well as interactions in nonlinear models for complex data sets. In a controlled simulation setting, we showed that using uncertainty-aware sensitivity is beneficial in the presence of uncertainty when the used model may be wrong. Moreover, the proposed methods were equally good or better than previous derivative based sensitivity analysis methods in all of the tested cases. We can thus recommend using uncertainty-aware sensitivity analysis in modelling situations with little data and/or lots of uncertainty. We also demonstrated with two real data sets that our

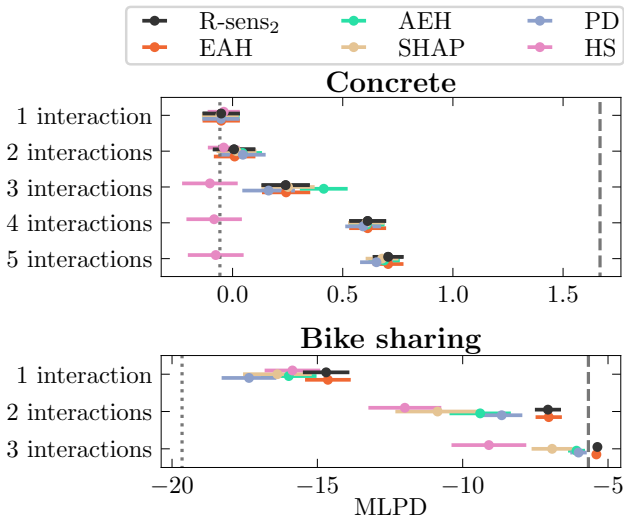


Figure 4: Mean log predictive densities (MLPDs) on independent test sets from the Concrete and Bike sharing data sets for Gaussian process models with different numbers of interactions. With each method, the interactions were identified from each training data set using the model with all interactions. The error bars represent 95% uncertainty intervals for the means from 50 different train-test splits. The dotted and dashed lines represent the MLPD for models with no interactions and all interactions, respectively.

proposed method identifies pairwise interactions in non-linear models that, when added to a model, improve its predictive performance. In addition, the ranking of the interactions between different Bootstrap samples of the data has less variation compared to many alternative variable importance methods.

Acknowledgements

We thank Alejandro Catalina and Kunal Ghosh for helpful comments to improve the manuscript. We thank Mostafa Abdelrahman for GPyTorch and autodiff implementations. We also acknowledge the computational resources provided by the Aalto Science-IT project and support by the Academy of Finland Flagship programme: Finnish Center for Artificial Intelligence, FCAI.

References

Baydin, A. G., Pearlmutter, B. A., Radul, A. A., and Siskind, J. M. (2018). Automatic differentiation in machine learning: a survey. *Journal of machine learning research*, 18(153).

Cacuci, D. G. (2003). *Sensitivity and Uncertainty*

Analysis, volume I: Theory. Boca Raton: Chapman and Hall/CRC.

Cacuci, D. G., Ionescu-Bujor, M., and Navon, I. M. (2005). *Sensitivity and uncertainty analysis, volume II: applications to large-scale systems*. CRC press.

Cui, T., Marttinen, P., and Kaski, S. (2020). Learning global pairwise interactions with bayesian neural networks. *Proceedings of the 24th European Conference on Artificial Intelligence (ECAI 2020)*.

Czernichow, T. (1996). Architecture selection through statistical sensitivity analysis. In *International Conference on Artificial Neural Networks*, pages 179–184. Springer.

Dorizzi, B. (1996). Variable selection using generalized RBF networks: Application to the forecast of the French T-bonds. *Proceedings of IEEE-IMACS'96, Lille, France*.

Fanaee-T, H. and Gama, J. (2014). Event labeling combining ensemble detectors and background knowledge. *Progress in Artificial Intelligence*, 2(2-3):113–127.

Fisher, A., Rudin, C., and Dominici, F. (2019). All models are wrong, but many are useful: Learning a variable’s importance by studying an entire class of prediction models simultaneously. *Journal of Machine Learning Research*, 20(177):1–81.

Friedman, J. H. (2001). Greedy function approximation: a gradient boosting machine. *Annals of statistics*, pages 1189–1232.

Friedman, J. H., Popescu, B. E., et al. (2008). Predictive learning via rule ensembles. *The Annals of Applied Statistics*, 2(3):916–954.

Fujimoto, K., Kojadinovic, I., and Marichal, J.-L. (2006). Axiomatic characterizations of probabilistic and cardinal-probabilistic interaction indices. *Games and Economic Behavior*, 55(1):72–99.

Gelman, A. and Pardoe, I. (2007). Average predictive comparisons for models with nonlinearity, interactions, and variance components. *Sociological Methodology*, 37(1):23–51.

Goldstein, A., Kapelner, A., Bleich, J., and Pitkin, E. (2015). Peeking inside the black box: Visualizing statistical learning with plots of individual conditional expectation. *Journal of Computational and Graphical Statistics*, 24(1):44–65.

Greenwell, B. M., Boehmke, B. C., and McCarthy, A. J. (2018). A simple and effective model-based variable importance measure. *arXiv preprint arXiv:1805.04755*.

Guidotti, R., Monreale, A., Ruggieri, S., Turini, F., Giannotti, F., and Pedreschi, D. (2018). A survey

- of methods for explaining black box models. *ACM computing surveys (CSUR)*, 51(5):1–42.
- Guyon, I. and Elisseeff, A. (2003). An introduction to variable and feature selection. *Journal of machine learning research*, 3(Mar):1157–1182.
- Hausler, D., Opper, M., et al. (1997). Mutual information, metric entropy and cumulative relative entropy risk. *The Annals of Statistics*, 25(6):2451–2492.
- Homma, T. and Saltelli, A. (1996). Importance measures in global sensitivity analysis of nonlinear models. *Reliability Engineering & System Safety*, 52(1):1–17.
- IM, S. (1993). Sensitivity estimates for nonlinear mathematical models. *Math. Model. Comput. Exp*, 1(4):407–414.
- Kendall, A. and Gal, Y. (2017). What uncertainties do we need in Bayesian deep learning for computer vision? In *Proceedings of the 31st International Conference on Neural Information Processing Systems*, pages 5580–5590.
- Kullback, S. (1959). *Statistics and information theory*. J. Wiley and Sons, New York.
- Kullback, S. and Leibler, R. A. (1951). On information and sufficiency. *The annals of mathematical statistics*, 22(1):79–86.
- Leray, P. and Gallinari, P. (1999). Feature selection with neural networks. *Behaviormetrika*, 26(1):145–166.
- Lundberg, S. M., Erion, G. G., and Lee, S.-I. (2018). Consistent individualized feature attribution for tree ensembles. *arXiv preprint arXiv:1802.03888*.
- MacKay, D. J. (1998). Introduction to Gaussian processes. In Bishop, J., editor, *Neural Networks and Machine Learning*, pages 133–166. Springer Verlag.
- Minka, T. P. (2001). *A family of algorithms for approximate Bayesian inference*. PhD thesis, Massachusetts Institute of Technology.
- Neal, R. (1998). Regression and classification using Gaussian process priors (with discussion). In Bernardo, J., Berger, J., Dawid, A., and Smith, A., editors, *Bayesian statistics*, volume 6, pages 475–501. Oxford University Press.
- Oakley, J. E. and O’Hagan, A. (2004). Probabilistic sensitivity analysis of complex models: a Bayesian approach. *Journal of the Royal Statistical Society: Series B (Statistical Methodology)*, 66(3):751–769.
- O’Hagan, A. (1978). Curve fitting and optimal design for prediction. *Journal of the Royal Statistical Society: Series B (Methodological)*, 40(1):1–24.
- O’Hagan, T. (2004). Dicing with the unknown. *Significance*, 1(3):132–133.
- Opper, M. and Winther, O. (2000). Gaussian processes for classification: Mean-field algorithms. *Neural Computation*, 12(11):2655–2684.
- Paananen, T., Piironen, J., Andersen, M. R., and Vehtari, A. (2019). Variable selection for Gaussian processes via sensitivity analysis of the posterior predictive distribution. volume 89 of *Proceedings of Machine Learning Research*, pages 1743–1752.
- Rasmussen, C. (2003). Gaussian processes to speed up hybrid monte carlo for expensive bayesian integrals. *Bayesian statistics*, 7:651–659.
- Rasmussen, C. E. and Williams, C. K. (2006). *Gaussian processes for machine learning*, volume 1. MIT press Cambridge.
- Refenes, A.-P. and Zaprani, A. (1999). Neural model identification, variable selection and model adequacy. *Journal of Forecasting*, 18(5):299–332.
- Rényi, A. et al. (1961). On measures of entropy and information. In *Proceedings of the Fourth Berkeley Symposium on Mathematical Statistics and Probability, Volume 1: Contributions to the Theory of Statistics*. The Regents of the University of California.
- Riihimäki, J., Sund, R., and Vehtari, A. (2010). Analysing the length of care episode after hip fracture: a nonparametric and a parametric Bayesian approach. *Health care management science*, 13(2):170–181.
- Ruck, D. W., Rogers, S. K., and Kabrisky, M. (1990). Feature selection using a multilayer perceptron. *Journal of Neural Network Computing*, 2(2):40–48.
- Saltelli, A. (2002). Sensitivity analysis for importance assessment. *Risk analysis*, 22(3):579–590.
- Shao, J. (2006). *Mathematical statistics: exercises and solutions*. Springer Science & Business Media.
- Shapley, L. S. (1953). A value for n-person games. *Contributions to the Theory of Games*, 2(28):307–317.
- Simonyan, K., Vedaldi, A., and Zisserman, A. (2013). Deep inside convolutional networks: Visualising image classification models and saliency maps. *arXiv preprint arXiv:1312.6034*.
- Solak, E., Murray-Smith, R., Leithead, W. E., Leith, D. J., and Rasmussen, C. E. (2003). Derivative observations in Gaussian process models of dynamic systems. In *Advances in neural information processing systems*, pages 1057–1064.
- Štrumbelj, E. and Kononenko, I. (2014). Explaining prediction models and individual predictions with feature contributions. *Knowledge and information systems*, 41(3):647–665.

- Sundararajan, M., Taly, A., and Yan, Q. (2017). Axiomatic attribution for deep networks. In *Proceedings of the 34th International Conference on Machine Learning*, pages 3319–3328.
- Van Erven, T. and Harremoës, P. (2014). Rényi divergence and Kullback-Leibler divergence. *IEEE Transactions on Information Theory*, 60(7):3797–3820.
- Walker, A. M. (1969). On the asymptotic behaviour of posterior distributions. *Journal of the Royal Statistical Society: Series B (Methodological)*, 31(1):80–88.
- Williams, C. K. and Barber, D. (1998). Bayesian classification with Gaussian processes. *IEEE Transactions on Pattern Analysis and Machine Intelligence*, 20(12):1342–1351.
- Yeh, I.-C. (2007). Modeling slump flow of concrete using second-order regressions and artificial neural networks. *Cement and concrete composites*, 29(6):474–480.
- Zeiler, M. D. and Fergus, R. (2014). Visualizing and understanding convolutional networks. In *European conference on computer vision*, pages 818–833. Springer.

5 R-SENS AND R-SENS₂ DERIVATIONS

5.1 R-sens

$$\begin{aligned}
 & \left. \frac{\partial^2 \mathcal{D}_\alpha [p(y^* | \boldsymbol{\lambda}^*(\mathbf{x}^*)) || p(y^* | \boldsymbol{\lambda}^*(\mathbf{x}^{**}))]}{(\partial x_d^{**})^2} \right|_{\mathbf{x}^{**}=\mathbf{x}^*} \\
 &= \left(\frac{\partial^2 \boldsymbol{\lambda}^*(\mathbf{x}^*)}{\partial x_d^2} \right)^T \left(\frac{\mathcal{D}_\alpha [p(y^* | \boldsymbol{\lambda}^*(\mathbf{x}^*)) || p(y^* | \boldsymbol{\lambda}^*(\mathbf{x}^{**}))]}{\partial \boldsymbol{\lambda}^*(\mathbf{x}^{**})} \right) \Big|_{\mathbf{x}^{**}=\mathbf{x}^*} + \\
 & \quad \left(\frac{\partial \boldsymbol{\lambda}^*(\mathbf{x}^*)}{\partial x_d^*} \right)^T \mathbf{H}_{\boldsymbol{\lambda}^*(\mathbf{x}^{**})} (\mathcal{D}_\alpha [p(y^* | \boldsymbol{\lambda}^*(\mathbf{x}^*)) || p(y^* | \boldsymbol{\lambda}^*(\mathbf{x}^{**}))]) \left(\frac{\partial \boldsymbol{\lambda}^*(\mathbf{x}^{**})}{\partial x_d^{**}} \right) \Big|_{\mathbf{x}^{**}=\mathbf{x}^*}, \\
 &= \mathbf{0} + \left(\frac{\partial \boldsymbol{\lambda}^*(\mathbf{x}^*)}{\partial x_d^*} \right)^T \mathbf{H}_{\boldsymbol{\lambda}^*(\mathbf{x}^{**})} (\mathcal{D}_\alpha [p(y^* | \boldsymbol{\lambda}^*(\mathbf{x}^*)) || p(y^* | \boldsymbol{\lambda}^*(\mathbf{x}^{**}))]) \left(\frac{\partial \boldsymbol{\lambda}^*(\mathbf{x}^{**})}{\partial x_d^{**}} \right) \Big|_{\mathbf{x}^{**}=\mathbf{x}^*}.
 \end{aligned} \tag{6}$$

5.2 R-sens₂

Here, we make the approximation that third and fourth derivatives of the Rényi divergence are zero. Let us start from the previous identity

$$\begin{aligned}
 & \left. \frac{\partial^2 \mathcal{D}_\alpha [p(y^* | \boldsymbol{\lambda}^*(\mathbf{x}^*)) || p(y^* | \boldsymbol{\lambda}^*(\mathbf{x}^{**}))]}{(\partial x_d^{**})^2} \right|_{\mathbf{x}^{**}=\mathbf{x}^*} \\
 &= \left(\frac{\partial \boldsymbol{\lambda}^*(\mathbf{x}^*)}{\partial x_d^*} \right)^T \mathbf{H}_{\boldsymbol{\lambda}^*(\mathbf{x}^{**})} (\mathcal{D}_\alpha [p(y^* | \boldsymbol{\lambda}^*(\mathbf{x}^*)) || p(y^* | \boldsymbol{\lambda}^*(\mathbf{x}^{**}))]) \left(\frac{\partial \boldsymbol{\lambda}^*(\mathbf{x}^{**})}{\partial x_d^{**}} \right) \Big|_{\mathbf{x}^{**}=\mathbf{x}^*} \\
 &= \sum_{k=1}^M \sum_{l=1}^M \frac{\partial^2 \mathcal{D}_\alpha [p(y^* | \boldsymbol{\lambda}^*) || p(y^* | \boldsymbol{\lambda}^*)]}{\partial \lambda_k^* \partial \lambda_l^*} \frac{\partial \lambda_k^*}{\partial x_d^*} \frac{\partial \lambda_l^*}{\partial x_d^*} \Big|_{\mathbf{x}^{**}=\mathbf{x}^*}.
 \end{aligned} \tag{7}$$

Then differentiating with respect to x_e gives the equality

$$\begin{aligned}
 & \left. \frac{\partial^3 \mathcal{D}_\alpha [p(y^* | \boldsymbol{\lambda}^*(\mathbf{x}^*)) || p(y^* | \boldsymbol{\lambda}^*(\mathbf{x}^{**}))]}{(\partial x_d^{**})^2 \partial x_e^{**}} \right|_{\mathbf{x}^{**}=\mathbf{x}^*} = \sum_{k=1}^M \sum_{l=1}^M \sum_{m=1}^M \frac{\partial^3 \mathcal{D}_\alpha [p(y^* | \boldsymbol{\lambda}^*) || p(y^* | \boldsymbol{\lambda}^*)]}{\partial \lambda_k^* \partial \lambda_l^* \partial \lambda_m^*} \frac{\partial \lambda_k^*}{\partial x_d^*} \frac{\partial \lambda_l^*}{\partial x_d^*} \frac{\partial \lambda_m^*}{\partial x_d^*} \\
 & + \sum_{k=1}^M \sum_{l=1}^M \frac{\partial^2 \mathcal{D}_\alpha [p(y^* | \boldsymbol{\lambda}^*) || p(y^* | \boldsymbol{\lambda}^*)]}{\partial \lambda_k^* \partial \lambda_l^*} \left(\frac{\partial^2 \lambda_k^*}{\partial x_d^* \partial x_e^*} \frac{\partial \lambda_l^*}{\partial x_d^*} + \frac{\partial \lambda_k^*}{\partial x_d^*} \frac{\partial^2 \lambda_l^*}{\partial x_d^* \partial x_e^*} \right) \\
 & = \sum_{k=1}^M \sum_{l=1}^M \frac{\partial^2 \mathcal{D}_\alpha [p(y^* | \boldsymbol{\lambda}^*) || p(y^* | \boldsymbol{\lambda}^*)]}{\partial \lambda_k^* \partial \lambda_l^*} \left(\frac{\partial^2 \lambda_k^*}{\partial x_d^* \partial x_e^*} \frac{\partial \lambda_l^*}{\partial x_d^*} + \frac{\partial \lambda_k^*}{\partial x_d^*} \frac{\partial^2 \lambda_l^*}{\partial x_d^* \partial x_e^*} \right).
 \end{aligned} \tag{8}$$

Differentiating a second time gives

$$\begin{aligned}
 & \left. \frac{\partial^4 \mathcal{D}_\alpha [p(y^* | \boldsymbol{\lambda}^*(\mathbf{x}^*)) || p(y^* | \boldsymbol{\lambda}^*(\mathbf{x}^{**}))]}{(\partial x_d^{**})^2 (\partial x_e^{**})^2} \right|_{\mathbf{x}^{**}=\mathbf{x}^*} \\
 &= \sum_{k=1}^M \sum_{l=1}^M \frac{\partial^2 \mathcal{D}_\alpha [p(y^* | \boldsymbol{\lambda}^*) || p(y^* | \boldsymbol{\lambda}^*)]}{\partial \lambda_k^* \partial \lambda_l^*} \left(\frac{\partial^3 \lambda_k^*}{\partial x_d^* \partial x_e^*} \frac{\partial \lambda_l^*}{\partial x_d^*} + \frac{\partial^2 \lambda_k^*}{\partial x_d^* \partial x_e^*} \frac{\partial^2 \lambda_l^*}{\partial x_d^* \partial x_e^*} + \frac{\partial^2 \lambda_k^*}{\partial x_d^* \partial x_e^*} \frac{\partial^2 \lambda_l^*}{\partial x_d^* \partial x_e^*} + \frac{\partial^2 \lambda_k^*}{\partial x_d^* \partial x_e^*} \frac{\partial^3 \lambda_l^*}{\partial x_d^* \partial x_e^* (\partial x_e^*)^2} \right).
 \end{aligned} \tag{9}$$

Dropping the third derivative terms and the factor 2 results in

$$\sum_{k=1}^M \sum_{l=1}^M \frac{\partial^2 \mathcal{D}_\alpha [p(y^* | \boldsymbol{\lambda}^*) || p(y^* | \boldsymbol{\lambda}^*)]}{\partial \lambda_k^* \partial \lambda_l^*} \frac{\partial^2 \lambda_k^*}{\partial x_d^* \partial x_e^*} \frac{\partial^2 \lambda_l^*}{\partial x_d^* \partial x_e^*} = \left(\frac{\partial^2 \boldsymbol{\lambda}^*}{\partial x_d^* \partial x_e^*} \right)^T \mathbf{H} (\mathcal{D}_\alpha [p(y^* | \boldsymbol{\lambda}^*) || p(y^* | \boldsymbol{\lambda}^*)]) \left(\frac{\partial^2 \boldsymbol{\lambda}^*}{\partial x_d^* \partial x_e^*} \right). \tag{10}$$

6 FINITE DIFFERENCE APPROXIMATION OF THE KULLBACK-LEIBLER DIVERGENCE

Consider two probability distributions, $p(\cdot|\boldsymbol{\lambda}^*)$ and $p(\cdot|\boldsymbol{\lambda}^{**})$ parameterised by vectors $\boldsymbol{\lambda}^*$ and $\boldsymbol{\lambda}^{**}$, respectively. Keeping $\boldsymbol{\lambda}^*$ constant, let us make a second-order approximation of the Kullback-Leibler divergence between the distributions in the neighbourhood around $\boldsymbol{\lambda}^{**} = \boldsymbol{\lambda}^*$.

$$\begin{aligned} & \mathcal{D}_{\text{KL}}(p(\cdot|\boldsymbol{\lambda}^*)||p(\cdot|\boldsymbol{\lambda}^{**})) \\ &= \mathcal{D}_{\text{KL}}(p(\cdot|\boldsymbol{\lambda}^*)||p(\cdot|\boldsymbol{\lambda}^{**})) \Big|_{\boldsymbol{\lambda}^{**}=\boldsymbol{\lambda}^*} + \sum_{k=1}^M (\lambda_k^{**} - \lambda_k^*) \frac{\partial \mathcal{D}_{\text{KL}}(p(\cdot|\boldsymbol{\lambda}^*)||p(\cdot|\boldsymbol{\lambda}^{**}))}{\partial \lambda_k^{**}} \Big|_{\boldsymbol{\lambda}^{**}=\boldsymbol{\lambda}^*} \\ &+ \frac{1}{2} \sum_{k=1}^M \sum_{l=1}^M \left[(\lambda_k^{**} - \lambda_k^*) (\lambda_l^{**} - \lambda_l^*) \frac{\partial^2 \mathcal{D}_{\text{KL}}(p(\cdot|\boldsymbol{\lambda}^*)||p(\cdot|\boldsymbol{\lambda}^{**}))}{\partial \lambda_k^{**} \partial \lambda_l^{**}} \Big|_{\boldsymbol{\lambda}^{**}=\boldsymbol{\lambda}^*} \right] + \mathcal{O}(\|\boldsymbol{\lambda}^{**} - \boldsymbol{\lambda}^*\|^3). \end{aligned}$$

The first two terms are zero, because the Kullback-Leibler divergence obtains a minimum value of zero at $\boldsymbol{\lambda}^{**} = \boldsymbol{\lambda}^*$. Dropping them and the third degree term, we are left with the approximation

$$\mathcal{D}_{\text{KL}}(p(\cdot|\boldsymbol{\lambda}^*)||p(\cdot|\boldsymbol{\lambda}^{**})) \approx \frac{1}{2} \sum_{k=1}^M \sum_{l=1}^M \left[(\lambda_k^{**} - \lambda_k^*) (\lambda_l^{**} - \lambda_l^*) \frac{\partial^2 \mathcal{D}_{\text{KL}}(p(\cdot|\boldsymbol{\lambda}^*)||p(\cdot|\boldsymbol{\lambda}^{**}))}{\partial \lambda_k^{**} \partial \lambda_l^{**}} \Big|_{\boldsymbol{\lambda}^{**}=\boldsymbol{\lambda}^*} \right].$$

If the distributions $p(\cdot|\boldsymbol{\lambda}^*)$ and $p(\cdot|\boldsymbol{\lambda}^{**})$ are predictive distributions, then the parameters $\boldsymbol{\lambda}^*$ and $\boldsymbol{\lambda}^{**}$ depend on the predictor value \mathbf{x} , i.e. $\boldsymbol{\lambda}^{**} = \boldsymbol{\lambda}(\mathbf{x}^{**})$. When only one predictor variable, x_d , is varied, an infinitesimal change in the parameters can be written as

$$\lambda_k^{**} - \lambda_k^* = \frac{\partial \lambda_k^{**}}{\partial x_d^{**}} (x_d^{**} - x_d^*).$$

Thus we get

$$\mathcal{D}_{\text{KL}}(p(\cdot|\boldsymbol{\lambda}^*)||p(\cdot|\boldsymbol{\lambda}^{**})) \approx \frac{1}{2} (x_d^{**} - x_d^*)^2 \sum_{k=1}^M \sum_{l=1}^M \left(\frac{\partial \lambda_k^{**}}{\partial x_d^{**}} \right) \left(\frac{\partial \lambda_l^{**}}{\partial x_d^{**}} \right) \frac{\partial^2 \mathcal{D}_{\text{KL}}(p(\cdot|\boldsymbol{\lambda}^*)||p(\cdot|\boldsymbol{\lambda}^{**}))}{\partial \lambda_k^{**} \partial \lambda_l^{**}} \Big|_{\boldsymbol{\lambda}^{**}=\boldsymbol{\lambda}^*}.$$

Rearranging the terms gives the approximate equivalence

$$\begin{aligned} \frac{2\mathcal{D}_{\text{KL}}(p(\cdot|\boldsymbol{\lambda}^*)||p(\cdot|\boldsymbol{\lambda}^{**}))}{(x_d^{**} - x_d^*)^2} &\approx \sum_{k=1}^M \sum_{l=1}^M \left(\frac{\partial \lambda_k^{**}}{\partial x_d^{**}} \right) \left(\frac{\partial \lambda_l^{**}}{\partial x_d^{**}} \right) \frac{\partial^2 \mathcal{D}_{\text{KL}}(p(\cdot|\boldsymbol{\lambda}^*)||p(\cdot|\boldsymbol{\lambda}^{**}))}{\partial \lambda_k^{**} \partial \lambda_l^{**}} \Big|_{\boldsymbol{\lambda}^{**}=\boldsymbol{\lambda}^*} \\ &= \frac{\partial^2 \mathcal{D}_{\text{KL}}(p(\cdot|\boldsymbol{\lambda}^*)||p(\cdot|\boldsymbol{\lambda}^{**}))}{(\partial x_d^{**})^2} \Big|_{\boldsymbol{\lambda}^{**}=\boldsymbol{\lambda}^*}. \end{aligned}$$

The last identity is based on the chain rule of differentiation. Finally, taking the square root gives the approximate equivalence

$$\frac{\sqrt{2\mathcal{D}_{\text{KL}}(p(\cdot|\boldsymbol{\lambda}^*)||p(\cdot|\boldsymbol{\lambda}^{**}))}}{|x_d^{**} - x_d^*|} \approx \sqrt{\frac{\partial^2 \mathcal{D}_{\text{KL}}(p(\cdot|\boldsymbol{\lambda}^*)||p(\cdot|\boldsymbol{\lambda}^{**}))}{(\partial x_d^{**})^2}} \Big|_{\boldsymbol{\lambda}^{**}=\boldsymbol{\lambda}^*},$$

where the left hand side is the finite difference KL method of Paananen et al. (2019) and the right hand side is the R-sens measure with $\alpha = 1$.

7 R-Sens₂ Approximation Benefits

In this section, we show an example of how the simplified R-sens₂ formula we use is better than the full formula that includes cross-derivative terms. With full formula we mean the fourth derivative of the Rényi divergence without dropping any terms. We replicate the simulation experiment from Section 3.2 of the main paper such that we compute interaction importance estimates using the simplified R-sens₂ formula and the full formula that is obtained with automatic differentiation. In Figure 5 we show the different interaction importances for a single simulation. The three annotated pairs are the true simulated interactions, whereas all the other interactions are irrelevant. The figure shows that the two formulas give almost equivalent importances for the true interactions, but the simplified formula gives much lower importance estimates for the irrelevant interactions, thus having significantly better ability to separate true interactions from nonexistent interactions.

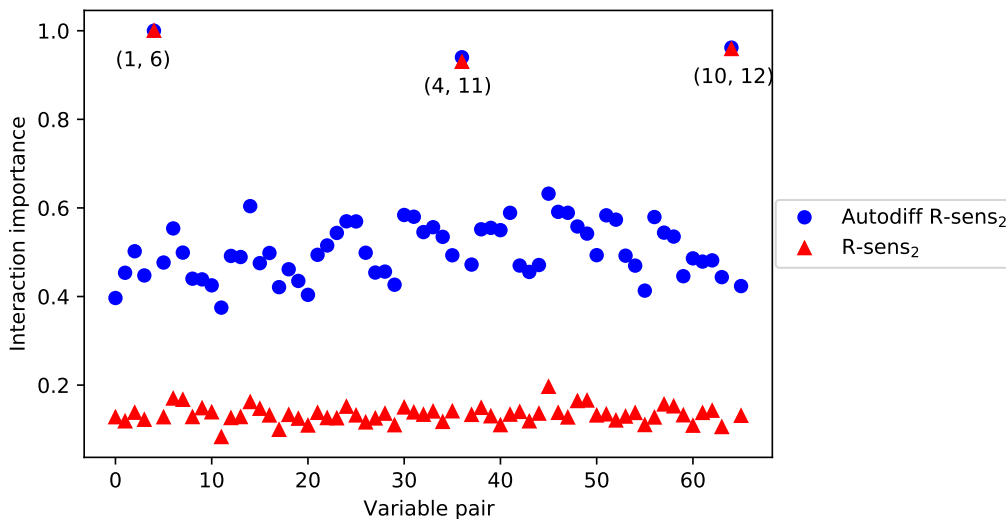


Figure 5: Comparison of interaction importance estimates for R-sens₂ (red) and the fourth derivative of the Rényi divergence (blue).

8 COMPUTATIONAL COST DETAILS

Here, we discuss the computational cost of the variable importance methods used in the main paper. Let us denote the number of observations with N and the number of predictor variables with D . Let us also denote the number of possible pairwise interactions with $\frac{D(D+1)}{2} \equiv D_2$. Let us denote the costs of making predictions from a regression model with a location-scale likelihood with

- C_E cost of $E[y]$,
- C_V cost of $\text{Var}[y]$,
- \tilde{C}_E cost of $\frac{\partial E[y]}{\partial x_d}$,
- \tilde{C}_V cost of $\frac{\partial \text{Var}[y]}{\partial x_d}$,
- \hat{C}_E cost of $\frac{\partial^2 E[y]}{\partial x_d^2}$,
- \hat{C}_V cost of $\frac{\partial^2 \text{Var}[y]}{\partial x_d^2}$.

The computational cost of the variable importance methods can be tuned based on the amount of computational resources. We tried to tune the cost of each method roughly equal in order to make the comparison fair. The computational costs that were used in the experiment of Section 3.1 in the main paper are shown in Table 3, and the costs used in the Concrete data experiment of Section 3.3 are shown in Table 4.



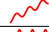
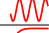

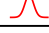



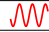


Table 3: Computational costs of the variable importance methods used in the first experiment of the main paper.

Method	Time complexity
R-sens	$ND(C_V + \tilde{C}_E + \tilde{C}_V)$
EAD	$ND\tilde{C}_E$
AED	$ND\tilde{C}_E$
APC	$2NDC_E + D^3$
SHAP	$2NDC_E$
PD	$9NDC_E$
PFI	$N(D+1)(C_E + C_V)$
VAR	$NDC_E + D^3$

Table 4: Computational costs of the variable importance methods (for interactions) used in the Concrete experiment of the main paper.

Method	Time complexity
R-sens	$ND_2(C_V + \hat{C}_E + \hat{C}_V)$
EAH	$ND_2\hat{C}_E$
AEH	$ND_2\hat{C}_E$
SHAP	$4ND_2C_E$
PD	$9ND_2C_E$
HS	$N^2D_2C_E$

Table 5: Average error in rankings in the simulated example of the main paper. Each predictor has an independent standard normal distribution.

Ground-truth models									
Function $f_{\text{true},i}(x)$	R-sens	EAD	AED	APC	SHAP	PD	PFI	VAR	
 x	0	0	0	0	0.9 ± 0.1	0.7 ± 0.1	1.0 ± 0.1	0.4 ± 0.1	
 x^3	0	0.0 ± 0.1	0.0 ± 0.1	5.9 ± 0.4	2.8 ± 0.2	3.3 ± 0.2	4.2 ± 0.3	2.0 ± 0.2	
 $x + \cos(3x)$	0	0.0 ± 0.0	3.9 ± 0.2	8.0 ± 0.3	0.8 ± 0.1	0.0 ± 0.1	0.7 ± 0.1	0.0 ± 0.1	
 $\sin(3x)$	0	0.0 ± 0.0	21.0 ± 0.6	10.8 ± 0.3	0.4 ± 0.1	0.1 ± 0.0	0.3 ± 0.1	3.2 ± 0.2	
 $x \exp(-x)$	0	0.4 ± 0.1	0.5 ± 0.1	7.9 ± 0.4	3.1 ± 0.3	1.6 ± 0.2	6.0 ± 0.3	2.2 ± 0.2	
 $\exp(-x^2)$	0	0.0 ± 0.0	20.5 ± 0.5	7.2 ± 0.3	0.5 ± 0.1	0.4 ± 0.1	0.4 ± 0.1	-0.1 ± 0.0	
Imperfect models									
Function $f_{\text{true},i}(x)$	R-sens	EAD	AED	APC	SHAP	PD	PFI	VAR	
 x	0	0.2 ± 0.1	0.1 ± 0.2	0.2 ± 0.2	1.3 ± 0.2	0.1 ± 0.1	1.9 ± 0.2	0.2 ± 0.1	
 x^3	0	0.2 ± 0.3	0.2 ± 0.3	6.2 ± 0.4	5.1 ± 0.4	2.0 ± 0.3	7.5 ± 0.5	1.1 ± 0.3	
 $x + \cos(3x)$	0	0.0 ± 0.1	4.0 ± 0.2	8.1 ± 0.3	1.5 ± 0.2	-0.1 ± 0.1	1.7 ± 0.2	0.0 ± 0.1	
 $\sin(3x)$	0	0.0 ± 0.0	20.9 ± 0.5	10.4 ± 0.3	0.4 ± 0.1	0.1 ± 0.1	0.4 ± 0.1	3.2 ± 0.2	
 $x \exp(-x)$	0	0.5 ± 0.3	0.7 ± 0.3	8.3 ± 0.5	5.8 ± 0.4	2.8 ± 0.4	10.0 ± 0.5	2.6 ± 0.3	
 $\exp(-x^2)$	0	0.0 ± 0.0	20.5 ± 0.5	7.2 ± 0.3	0.5 ± 0.1	0.5 ± 0.1	0.4 ± 0.1	-0.1 ± 0.0	




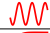

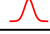



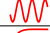
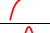

9 SIMULATED INDIVIDUAL EFFECTS - ADDITIONAL RESULTS

9.1 Different Distributions for the Predictors

9.1.1 Gaussian





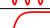
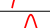




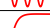
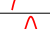
9.1.2 Mixture of 2 Gaussians

Table 6: Average error in rankings in the simulated example of the main paper. Each predictor is independently distributed with a mixture of 2 Gaussians.

Ground-truth models									
Function $f_{\text{true},i}(x)$	R-sens	EAD	AED	APC	SHAP	PD	PFI	VAR	
 x	0	0.0 ± 0.0	0.0 ± 0.0	0.0 ± 0.0	0.5 ± 0.1	0.1 ± 0.0	0.4 ± 0.1	0.0 ± 0.0	
 x^3	0	0.0 ± 0.0	0.0 ± 0.0	6.6 ± 0.4	1.6 ± 0.2	1.4 ± 0.1	2.0 ± 0.2	1.0 ± 0.1	
 $x + \cos(3x)$	0	0.0 ± 0.0	3.8 ± 0.2	6.5 ± 0.3	0.6 ± 0.1	0.1 ± 0.1	0.5 ± 0.1	-0.1 ± 0.0	
 $\sin(3x)$	0	0.0 ± 0.0	3.6 ± 0.2	8.1 ± 0.3	0.5 ± 0.1	0.1 ± 0.1	0.3 ± 0.1	2.3 ± 0.2	
 $x \exp(-x)$	0	0.1 ± 0.1	0.2 ± 0.1	8.2 ± 0.4	1.2 ± 0.2	0.5 ± 0.2	1.8 ± 0.2	2.5 ± 0.2	
 $\exp(-x^2)$	0	0.0 ± 0.0	20.4 ± 0.5	9.8 ± 0.4	0.7 ± 0.1	0.3 ± 0.1	0.6 ± 0.1	0.0 ± 0.0	
Imperfect models									
Function $f_{\text{true},i}(x)$	R-sens	EAD	AED	APC	SHAP	PD	PFI	VAR	
 x	0	0.1 ± 0.2	0.2 ± 0.2	-0.6 ± 0.1	-0.0 ± 0.2	-0.8 ± 0.1	-0.2 ± 0.1	-0.7 ± 0.1	
 x^3	0	0.1 ± 0.2	0.1 ± 0.2	6.0 ± 0.4	1.4 ± 0.2	0.4 ± 0.2	2.5 ± 0.2	1.3 ± 0.2	
 $x + \cos(3x)$	0	0.0 ± 0.1	3.9 ± 0.2	6.6 ± 0.3	0.7 ± 0.1	-0.1 ± 0.1	0.7 ± 0.1	-0.3 ± 0.1	
 $\sin(3x)$	0	0.0 ± 0.0	3.7 ± 0.2	7.7 ± 0.3	0.5 ± 0.1	0.1 ± 0.1	0.4 ± 0.1	1.9 ± 0.2	
 $x \exp(-x)$	0	0.1 ± 0.2	0.2 ± 0.2	7.8 ± 0.4	1.1 ± 0.3	0.0 ± 0.2	2.6 ± 0.3	3.9 ± 0.3	
 $\exp(-x^2)$	0	0.0 ± 0.0	20.4 ± 0.5	9.3 ± 0.4	0.7 ± 0.1	0.3 ± 0.1	0.6 ± 0.1	0.0 ± 0.0	

9.1.3 Correlated Gaussian

Table 7: Average error in rankings in the simulated example of the main paper. The predictors have a multivariate Normal distribution with all correlations 0.8.

Ground-truth models									
Function $f_{\text{true},i}(x)$	R-sens	EAD	AED	APC	SHAP	PD	PFI	VAR	
 x	0	0.0 ± 0.0	0.0 ± 0.0	0.0 ± 0.0	0.5 ± 0.1	0.1 ± 0.0	3.5 ± 0.2	0.4 ± 0.1	
 x^3	0	0.0 ± 0.0	0.0 ± 0.0	4.6 ± 0.4	2.6 ± 0.2	2.8 ± 0.2	5.2 ± 0.3	1.1 ± 0.1	
 $x + \cos(3x)$	0	0.0 ± 0.0	3.4 ± 0.2	6.1 ± 0.3	0.5 ± 0.1	-0.1 ± 0.1	2.5 ± 0.2	-0.1 ± 0.1	
 $\sin(3x)$	0	0.0 ± 0.0	20.8 ± 0.5	7.4 ± 0.3	0.5 ± 0.1	0.1 ± 0.0	1.0 ± 0.1	0.0 ± 0.0	
 $x \exp(-x)$	0	0.2 ± 0.1	0.3 ± 0.1	4.4 ± 0.3	3.1 ± 0.2	1.6 ± 0.2	6.7 ± 0.3	1.4 ± 0.2	
 $\exp(-x^2)$	0	0.0 ± 0.0	18.9 ± 0.6	4.6 ± 0.3	0.4 ± 0.1	0.1 ± 0.1	2.1 ± 0.2	0.0 ± 0.0	
Imperfect models									
Function $f_{\text{true},i}(x)$	R-sens	EAD	AED	APC	SHAP	PD	PFI	VAR	
 x	0	0.2 ± 0.1	0.2 ± 0.1	1.3 ± 0.2	0.7 ± 0.2	-0.4 ± 0.1	4.3 ± 0.3	-0.0 ± 0.1	
 x^3	0	0.1 ± 0.3	0.1 ± 0.3	6.4 ± 0.4	3.8 ± 0.4	1.4 ± 0.3	9.5 ± 0.8	0.5 ± 0.3	
 $x + \cos(3x)$	0	0.0 ± 0.1	3.4 ± 0.2	6.6 ± 0.3	1.0 ± 0.1	-0.2 ± 0.1	3.2 ± 0.2	-0.3 ± 0.1	
 $\sin(3x)$	0	0.0 ± 0.0	20.7 ± 0.5	7.5 ± 0.3	0.5 ± 0.1	0.0 ± 0.1	1.0 ± 0.1	-0.1 ± 0.0	
 $x \exp(-x)$	0	0.4 ± 0.3	0.5 ± 0.3	5.7 ± 0.4	4.8 ± 0.4	3.2 ± 0.5	11.1 ± 0.8	1.9 ± 0.3	
 $\exp(-x^2)$	0	0.0 ± 0.0	18.9 ± 0.6	4.6 ± 0.3	0.5 ± 0.1	0.1 ± 0.1	2.1 ± 0.2	0.0 ± 0.0	

10 R-SENS FOR GAUSSIAN PROCESS MODELS

Gaussian process models are widely used in supervised learning, where the task is to predict an output y from a D -dimensional input \mathbf{x} . The type of functions the Gaussian process can represent are determined by its covariance function, which is a key decision made during modelling. The covariance function $k(\mathbf{x}^{(i)}, \mathbf{x}^{(j)})$ defines the covariance between the function values at the input points $\mathbf{x}^{(i)}$ and $\mathbf{x}^{(j)}$. We assume the Gaussian process has a zero mean, in which case the joint distribution of the latent output values f at the training points is

$$p(f(\mathbf{X})) = p(\mathbf{f}) = \text{Normal}(\mathbf{f} | 0, \mathbf{K}),$$

where \mathbf{K} is the covariance matrix between the latent function values at the training inputs $\mathbf{X} = (\mathbf{x}^{(1)}, \dots, \mathbf{x}^{(N)})$ such that $\mathbf{K}_{ij} = k(\mathbf{x}^{(i)}, \mathbf{x}^{(j)})$.

In this work, we use the exponentiated quadratic covariance function

$$k_{\text{EQ}}(\mathbf{x}^{(i)}, \mathbf{x}^{(j)}) = \sigma_f^2 \exp \left(-\frac{1}{2} \sum_{k=1}^D \frac{(x_k^{(i)} - x_k^{(j)})^2}{l_k^2} \right). \quad (11)$$

Here, the hyperparameter σ_f determines the overall variability of the functions, and (l_1, \dots, l_D) are the length-scales of each input dimension. By defining an observation model that links the observations to the latent values of the Gaussian process, the model can be used for inference and predictions in many supervised learning tasks.

For example, in regression with an assumption of Gaussian noise, the posterior distribution of latent values for a new input point \mathbf{x}^* is a univariate normal distribution with mean and variance

$$\begin{aligned} \mathbb{E}[f^* | \mathbf{x}^*, \mathbf{y}] &= k(\mathbf{x}^*, \mathbf{X})(k(\mathbf{X}, \mathbf{X}) + \sigma^2 \mathbf{I})^{-1} \mathbf{y} \\ \text{Var}[f^* | \mathbf{x}^*, \mathbf{y}] &= k(\mathbf{x}^*, \mathbf{x}^*) - k(\mathbf{x}^*, \mathbf{X})(k(\mathbf{X}, \mathbf{X}) + \sigma^2 \mathbf{I})^{-1} k(\mathbf{X}, \mathbf{x}^*), \end{aligned} \quad (12)$$

where σ^2 is the noise variance, \mathbf{I} is the identity matrix, and \mathbf{y} is the vector of training outputs. For many other observation models, the posterior of latent values is not Gaussian, but it is commonplace to approximate it with a Gaussian distribution during inference, and many methods have been developed for doing so (Williams and Barber, 1998; Opper and Winther, 2000; Minka, 2001; Rasmussen and Williams, 2006). The variable importance assessment thus depends implicitly on the posterior approximation, as does any general method that uses the model's predictions.

10.1 Differentiating Gaussian Processes

We assume that the posterior distribution of latent values is Gaussian. Because differentiation is a linear operation, the derivatives of the parameters of a Gaussian process posterior distribution with respect to predictor variables are available in closed form (Solak et al., 2003; Rasmussen, 2003). For example, for the Gaussian observation model, the derivatives of the mean and variance of the predictive distribution in equation (12) with respect to the predictor variable x_d at point \mathbf{x}^* are given as

$$\begin{aligned} \frac{\partial \mathbb{E}[f^* | \mathbf{x}^*, \mathbf{y}]}{\partial x_d^*} &= \frac{\partial k(\mathbf{x}^*, \mathbf{X})}{\partial x_d^*} (k(\mathbf{X}, \mathbf{X}) + \sigma^2 \mathbf{I})^{-1} \mathbf{y} \\ \frac{\partial \text{Var}[f^* | \mathbf{x}^*, \mathbf{y}]}{\partial x_d^*} &= \frac{\partial k(\mathbf{x}^*, \mathbf{x}^*)}{\partial x_d^*} - \frac{\partial k(\mathbf{x}^*, \mathbf{X})}{\partial x_d^*} (k(\mathbf{X}, \mathbf{X}) + \sigma^2 \mathbf{I})^{-1} k(\mathbf{X}, \mathbf{x}^*) - k(\mathbf{x}^*, \mathbf{X})(k(\mathbf{X}, \mathbf{X}) + \sigma^2 \mathbf{I})^{-1} \frac{\partial k(\mathbf{X}, \mathbf{x}^*)}{\partial x_d^*}. \end{aligned}$$

For the exponentiated quadratic covariance function in equation (11), the partial derivatives with respect to the predictor variable x_d are

$$\begin{aligned} \frac{\partial k_{\text{EQ}}(\mathbf{x}^{(i)}, \mathbf{x}^{(j)})}{\partial x_d^{(i)}} &= \sigma_f^2 \exp \left(-\frac{1}{2} \sum_{k=1}^D \frac{(x_k^{(i)} - x_k^{(j)})^2}{l_k^2} \right) \left(-\frac{x_d^{(i)} - x_d^{(j)}}{l_d^2} \right), \\ \frac{\partial k_{\text{EQ}}(\mathbf{x}^{(i)}, \mathbf{x}^{(j)})}{\partial x_d^{(j)}} &= -\frac{\partial k_{\text{EQ}}(\mathbf{x}^{(i)}, \mathbf{x}^{(j)})}{\partial x_d^{(i)}}. \end{aligned}$$

The second derivatives are

$$\frac{\partial^2 k_{\text{EQ}}(\mathbf{x}^{(i)}, \mathbf{x}^{(j)})}{\partial x_d^{(i)} \partial x_e^{(i)}} = \frac{\partial^2 k_{\text{EQ}}(\mathbf{x}^{(i)}, \mathbf{x}^{(j)})}{\partial x_d^{(j)} \partial x_e^{(j)}} = \sigma_f^2 \exp\left(-\frac{1}{2} \sum_{k=1}^D \frac{(x_k^{(i)} - x_k^{(j)})^2}{l_k^2}\right) \left(\frac{x_d^{(i)} - x_d^{(j)}}{l_d^2}\right) \left(\frac{x_e^{(i)} - x_e^{(j)}}{l_e^2}\right).$$

For the R-sens measure, we need derivatives with respect to the parameters of the predictive distribution and not the posterior of the latent values. However, for many observation models these are obtained as a function of the derivatives of the latent values. In this section, we derive the equations for some commonly used observation models.

10.2 Regression with Gaussian Observation Model

In regression problems, it is commonly assumed that the noise has a Gaussian distribution. For a Gaussian observation model, the predictive distribution for a new observation y^* at a single predictor value \mathbf{x}^* is a normal distribution, which we will denote

$$p(y^* | \mathbf{x}^*, \mathbf{y}) = \text{Normal}(y^* | \mathbb{E}[y^*], \text{Var}[y^*]) = \text{Normal}(y^* | \mathbb{E}[f^*], \text{Var}[f^*] + \sigma^2),$$

where $\mathbb{E}[f^*]$ and $\text{Var}[f^*]$ are the mean and variance of the posterior distribution of latent values at \mathbf{x}^* , and σ^2 is the noise variance. Now, the derivatives of $\mathbb{E}[y^*]$ and $\text{Var}[y^*]$ with respect to predictor variable x_d^* are simply

$$\begin{aligned} \frac{\partial \mathbb{E}[y^*]}{\partial x_d^*} &= \frac{\partial \mathbb{E}[f^*]}{\partial x_d^*} \\ \frac{\partial \text{Var}[y^*]}{\partial x_d^*} &= \frac{\partial \text{Var}[f^*]}{\partial x_d^*} \\ \frac{\partial^2 \mathbb{E}[y^*]}{\partial x_d^* \partial x_e^*} &= \frac{\partial^2 \mathbb{E}[f^*]}{\partial x_d^* \partial x_e^*} \\ \frac{\partial^2 \text{Var}[y^*]}{\partial x_d^* \partial x_e^*} &= \frac{\partial^2 \text{Var}[f^*]}{\partial x_d^* \partial x_e^*}. \end{aligned}$$

The Fisher information elements of the normal distribution are

$$\begin{aligned} \mathcal{I}_N(\mathbb{E}[y^*]) &= \frac{1}{\text{Var}[y^*]} \\ \mathcal{I}_N(\text{Var}[y^*]) &= \frac{1}{2(\text{Var}[y^*])^2}. \end{aligned}$$

Thus, the R-sens measure takes the form

$$\text{R-sens}(x_d, \alpha = 1) = \sqrt{\frac{1}{\text{Var}[y^*]} \left(\frac{\partial \mathbb{E}[f^*]}{\partial x_d^*}\right)^2 + \frac{1}{2(\text{Var}[y^*])^2} \left(\frac{\partial \text{Var}[f^*]}{\partial x_d^*}\right)^2}.$$

Here, the first term is proportional to the slope of the mean prediction scaled by the predictive uncertainty, as with the linear regression model discussed in Section 2.1 of the main paper. The R-sens_2 measure evaluates to

$$\text{R-sens}_2(x_d, x_e, \alpha = 1) = \sqrt{\frac{1}{\text{Var}[y^*]} \left(\frac{\partial^2 \mathbb{E}[f^*]}{\partial x_d^* \partial x_e^*}\right)^2 + \frac{1}{2(\text{Var}[y^*])^2} \left(\frac{\partial^2 \text{Var}[f^*]}{\partial x_d^* \partial x_e^*}\right)^2}.$$

10.3 Binary Classification

For binary classification problems, the predictive distribution is a Bernoulli distribution with only one parameter, the probability of positive classification. This is obtained by squashing the latent Gaussian process function through a link function and integrating over the posterior of the latent function values. Two commonly used link functions for Gaussian process classification are the logit and probit. The Probit link function has the benefit that the predictive distribution has an analytical formula when the posterior distribution of latent values is

approximated with a Gaussian. Using a Probit link function, the predictive probability has thus an approximate analytical form

$$\pi^* = p(y = 1 | \mathbf{x}^*, \mathbf{y}) = \Phi \left(\frac{\mathbb{E}[f^*]}{\sqrt{1 + \text{Var}[f^*]}} \right),$$

where Φ is the cumulative distribution of the standard normal distribution.

Now, the derivatives of π^* with respect to x_d^* are

$$\begin{aligned} \frac{\partial \pi^*}{\partial x_d^*} &= \text{Normal} \left(\frac{\mathbb{E}[f^*]}{\sqrt{1 + \text{Var}[f^*]}} \right) \left[\frac{1}{\sqrt{1 + \text{Var}[f^*]}} \frac{\partial \mathbb{E}[f^*]}{\partial x_d^*} - \frac{\mathbb{E}[f^*]}{2(1 + \text{Var}[f^*])^{3/2}} \frac{\partial \text{Var}[f^*]}{\partial x_d^*} \right], \\ \frac{\partial^2 \pi^*}{\partial x_d^* \partial x_e^*} &= \text{Normal} \left(\frac{\mathbb{E}[f^*]}{\sqrt{1 + \text{Var}[f^*]}} \right) \left(\frac{\mathbb{E}[f^*]}{\sqrt{1 + \text{Var}[f^*]}} \right) \left[\frac{1}{\sqrt{1 + \text{Var}[f^*]}} \frac{\partial \mathbb{E}[f^*]}{\partial x_d^*} - \frac{\mathbb{E}[f^*]}{2(1 + \text{Var}[f^*])^{3/2}} \frac{\partial \text{Var}[f^*]}{\partial x_d^*} \right] \times \\ &\quad \left[\frac{1}{\sqrt{1 + \text{Var}[f^*]}} \frac{\partial \mathbb{E}[f^*]}{\partial x_e^*} - \frac{\mathbb{E}[f^*]}{2(1 + \text{Var}[f^*])^{3/2}} \frac{\partial \text{Var}[f^*]}{\partial x_e^*} \right] + \\ &\quad \text{Normal} \left(\frac{\mathbb{E}[f^*]}{\sqrt{1 + \text{Var}[f^*]}} \right) \left[\frac{1}{\sqrt{1 + \text{Var}[f^*]}} \frac{\partial^2 \mathbb{E}[f^*]}{\partial x_d^* \partial x_e^*} - \frac{\partial \mathbb{E}[f^*]}{\partial x_d^*} \frac{1}{2(1 + \text{Var}[f^*])^{3/2}} \frac{\partial \text{Var}[f^*]}{\partial x_e^*} \right. \\ &\quad \left. - \frac{\partial^2 \text{Var}[f^*]}{\partial x_d^* \partial x_e^*} \frac{\mathbb{E}[f^*]}{2(1 + \text{Var}[f^*])^{3/2}} - \frac{\partial \text{Var}[f^*]}{\partial x_d^*} \left(\frac{\partial \mathbb{E}[f^*]}{\partial x_e^*} \frac{1}{2(1 + \text{Var}[f^*])^{3/2}} - \frac{3\mathbb{E}[f^*]}{4(1 + \text{Var}[f^*])^{3/2}} \frac{\partial \text{Var}[f^*]}{\partial x_e^*} \right) \right]. \end{aligned}$$

The Fisher information of the Bernoulli distribution is

$$\mathcal{I}_{\text{Bern}}(\pi^*) = \frac{1}{\pi^*(1 - \pi^*)} = \left(\Phi \left(\frac{\mathbb{E}[f^*]}{\sqrt{1 + \text{Var}[f^*]}} \right) \right)^{-1} \left(1 - \Phi \left(\frac{\mathbb{E}[f^*]}{\sqrt{1 + \text{Var}[f^*]}} \right) \right)^{-1}.$$

The R-sens and R-sens₂ measures take the form

$$\begin{aligned} \text{R-sens}(\mathbf{x}^*, x_d, \alpha = 1) &= \sqrt{\mathcal{I}_{\text{Bern}}(\pi^*) \left(\frac{\partial \pi^*}{\partial x_d^*} \right)^2}, \\ \text{R-sens}_2(\mathbf{x}^*, (x_d, x_e), \alpha = 1) &= \sqrt{\mathcal{I}_{\text{Bern}}(\pi^*) \left(\frac{\partial^2 \pi^*}{\partial x_d^* \partial x_e^*} \right)^2}. \end{aligned}$$

10.4 Poisson Observation Model

For modelling count data with Gaussian processes, it is common to use a combination of a count observation model with a link function that transforms the positively constrained parameters to unconstrained scale where the Gaussian Process prior is placed. Here, we derive the equations needed for the R-sens method for the case of Poisson likelihood and exponential link function.

The likelihood is

$$p(\mathbf{y} | \mathbf{f}) = \prod_{i=1}^n \text{Poisson}(y_i | \lambda_i(f_i)) = \prod_{i=1}^n \text{Poisson}(y_i | \exp(f_i)).$$

Now, the Gaussian process prior is placed on the unconstrained latent values. If one uses a Gaussian approximation to the posterior of the latent values, then the transformed λ 's have a log-normal distribution. The intensity λ at any input point is given by integrating over the approximate posterior $q(f^* | \mathbf{y}, \mathbf{x}^*)$

$$\lambda^* = \int \exp(f^*) q(f^* | \mathbf{y}, \mathbf{x}^*) df^*.$$

This evaluates to the mean of the log-normal distribution

$$\lambda^* = \mathbb{E}[\text{Lognormal}(\mathbb{E}[f^*], \text{Var}[f^*])] = \exp(\mathbb{E}[f^*] + \text{Var}[f^*]/2).$$

The derivatives of this with respect to the predictor variables are

$$\begin{aligned} \frac{\partial \lambda^*}{\partial x_d^*} &= \exp(\mathbb{E}[f^*] + \text{Var}[f^*]/2) \left(\frac{\partial \mathbb{E}[f^*]}{\partial x_d^*} + \frac{1}{2} \frac{\partial \text{Var}[f^*]}{\partial x_d^*} \right), \\ \frac{\partial^2 \lambda^*}{\partial x_d^* \partial x_e^*} &= \exp(\mathbb{E}[f^*] + \text{Var}[f^*]/2) \times \\ &\left[\left(\frac{\partial \mathbb{E}[f^*]}{\partial x_d^*} + \frac{1}{2} \frac{\partial \text{Var}[f^*]}{\partial x_d^*} \right) \left(\frac{\partial \mathbb{E}[f^*]}{\partial x_e^*} + \frac{1}{2} \frac{\partial \text{Var}[f^*]}{\partial x_e^*} \right) + \left(\frac{\partial^2 \mathbb{E}[f^*]}{\partial x_d^* \partial x_e^*} + \frac{1}{2} \frac{\partial^2 \text{Var}[f^*]}{\partial x_d^* \partial x_e^*} \right) \right]. \end{aligned}$$

The Fisher information of the Poisson distribution is

$$\mathcal{I}_{\text{Pois}}(\lambda^*) = \frac{1}{\lambda^*} = \frac{1}{\exp(\mathbb{E}[f^*] + \text{Var}[f^*]/2)}.$$

Thus, the R-sens and R-sens₂ measures take the form

$$\text{R-sens}(\mathbf{x}^*, x_d, \alpha = 1) = \sqrt{\exp\left(\mathbb{E}[f^*] + \frac{\text{Var}[f^*]}{2}\right) \left| \frac{\partial \mathbb{E}[f^*]}{\partial x_d^*} + \frac{1}{2} \frac{\partial \text{Var}[f^*]}{\partial x_d^*} \right|},$$

$$\text{R-sens}_2(\mathbf{x}^*, (x_d, x_e), \alpha = 1)$$

$$= \sqrt{\exp\left(\mathbb{E}[f^*] + \frac{\text{Var}[f^*]}{2}\right) \left| \left(\frac{\partial \mathbb{E}[f^*]}{\partial x_d^*} + \frac{1}{2} \frac{\partial \text{Var}[f^*]}{\partial x_d^*} \right) \left(\frac{\partial \mathbb{E}[f^*]}{\partial x_e^*} + \frac{1}{2} \frac{\partial \text{Var}[f^*]}{\partial x_e^*} \right) + \left(\frac{\partial^2 \mathbb{E}[f^*]}{\partial x_d^* \partial x_e^*} + \frac{1}{2} \frac{\partial^2 \text{Var}[f^*]}{\partial x_d^* \partial x_e^*} \right) \right|}.$$

11 ILLUSTRATIVE EXAMPLE - LOGISTIC REGRESSION

In this section, we show an illustrative example similar to the main paper, but with a logistic regression model where the target variable y is binary. As the inverse link function, we use the cumulative Normal distribution. We consider a simple multivariate Gaussian prior on the regression coefficients. Contrary to the linear regression example, the posterior distribution has no closed form. We will use the Laplace approximation to get a Gaussian approximation to the posterior. The approximate posterior is

$$p(\boldsymbol{\beta}|\mathbf{X}, \mathbf{y}) \approx \mathcal{N}(\hat{\boldsymbol{\beta}}, \mathbf{H}^{-1}),$$

where $\hat{\boldsymbol{\beta}}$ is the maximum a posteriori estimate of the regression coefficients. When using the inverse cumulative Normal distribution as the link function, the predictive distribution at a new point \mathbf{x}^* has a closed form equation.

$$p(y^* = 1|\mathbf{x}^*, \mathbf{X}, \mathbf{y}) = \pi^*(\mathbf{x}^*) = \Phi\left(\frac{\mathbf{x}^* \hat{\boldsymbol{\beta}}}{\sqrt{1 + \mathbf{x}^* (\mathbf{H})^{-1} \mathbf{x}^{*T}}}\right).$$

The derivative of the success probability is

$$\frac{\partial \pi^*(\mathbf{x}^*)}{\partial x_d^*} = \mathcal{N}\left(\frac{\mathbf{x}^* \hat{\boldsymbol{\beta}}}{\sqrt{1 + \mathbf{x}^* (\mathbf{H})^{-1} \mathbf{x}^{*T}}}\right) \left[\frac{\hat{\beta}_d}{\sqrt{1 + \mathbf{x}^* (\mathbf{H})^{-1} \mathbf{x}^{*T}}} - \frac{\mathbf{x}^* \hat{\boldsymbol{\beta}} [(\mathbf{H})^{-1} \mathbf{x}^{*T}]_d}{(1 + \mathbf{x}^* (\mathbf{H})^{-1} \mathbf{x}^{*T})^{3/2}} \right].$$

The Fisher information of the Bernoulli distribution is

$$\mathcal{I}_{\text{Ber}}(\pi^*) = \frac{1}{\pi^*(1 - \pi^*)}.$$

The R-sens sensitivity measure for variable x_d^* thus evaluates to

$$\sqrt{\frac{1}{\pi^*(1 - \pi^*)}} \mathcal{N}\left(\frac{\mathbf{x}^* \hat{\boldsymbol{\beta}}}{\sqrt{1 + \mathbf{x}^* (\mathbf{H})^{-1} \mathbf{x}^{*T}}}\right) \left| \frac{\hat{\beta}_d}{\sqrt{1 + \mathbf{x}^* (\mathbf{H})^{-1} \mathbf{x}^{*T}}} - \frac{\mathbf{x}^* \hat{\boldsymbol{\beta}} [(\mathbf{H})^{-1} \mathbf{x}^{*T}]_d}{(1 + \mathbf{x}^* (\mathbf{H})^{-1} \mathbf{x}^{*T})^{3/2}} \right|. \quad (13)$$

To illustrate the R-sens measure in equation (13), we simulated 1000 observations from a logistic regression model with two predictor variables x_1 and x_2 whose true regression coefficients are $\beta_1 = 1$ and $\beta_2 = 0$. The predictor variables are independent and normally distributed with zero mean and standard deviation one. The R-sens sensitivities for both variables given by equation (13) are shown in Figure 6. The dashed line shows the derivative of the prediction function without the Fisher information term. Because of the link function, this derivative is not constant and is much larger close to the decision boundary. The Fisher information term does not remove this effect, but gives a bit more weight to points further away.

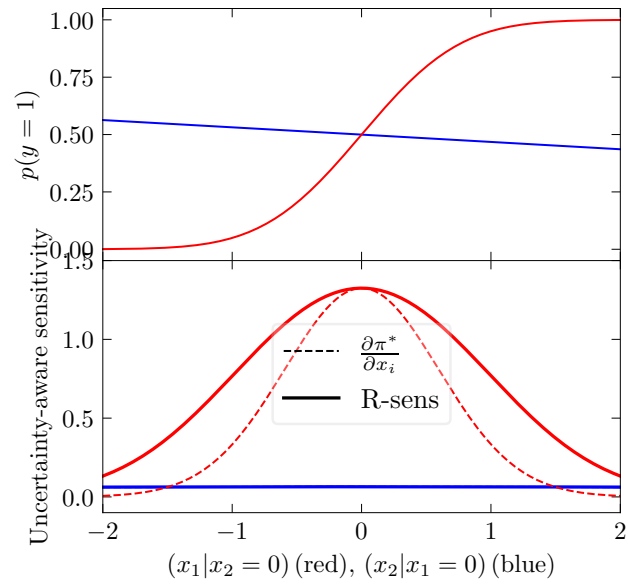


Figure 6: Top: Predictive distributions $p(y = 1 | x_1, x_2 = 0)$ (red) and $p(y = 1 | x_2, x_1 = 0)$ (blue) for the logistic regression model. Bottom: R-sens uncertainty-aware sensitivity measure given by equation (13) for x_1 (red) and x_2 (blue).

12 ASYMPTOTIC RESULTS FOR GENERALISED LINEAR MODELS

In Section 2.1 in the main paper, we discussed the behaviour of the posterior predictive distribution for a Bayesian linear regression model as the number of observations goes to infinity. In this case, the predictive uncertainty tends to a constant, and the R-sens local sensitivity measure for each predictor is proportional the absolute value of the maximum likelihood estimate of the regression coefficient, $|\hat{\beta}_d|$. In this section we discuss the asymptotic results of the logistic and Poisson regression models, which are nonlinear models that can be used to model binary or integer data.

12.1 Logistic Regression Model

12.1.1 Logit Link Function

The predictive distribution of a logistic regression model is a Bernoulli distribution. In the asymptotic limit, the posterior of the regression coefficients concentrates to a point $\hat{\beta}$, and the “success probability” parameter as a function of the predictor variables is the logistic function

$$p(y^* = 1 | \mathbf{X}, \mathbf{y}, \mathbf{x}^*) := \pi^*(\mathbf{x}^*) = \frac{\exp(\mathbf{x}^* \hat{\beta})}{1 + \exp(\mathbf{x}^* \hat{\beta})}.$$

The derivative of π^* with respect to x_d^* is

$$\frac{\partial \pi^*}{\partial x_d^*} = \hat{\beta}_d \pi^* (1 - \pi^*).$$

The Fisher information of the Bernoulli distribution

$$\mathcal{I}_{\text{bern}}(\pi^*) = \frac{1}{\pi^*(1 - \pi^*)}.$$

In the limit when the number of observations goes to infinity, the R-sens measure thus evaluates to

$$\sqrt{\mathcal{I}_{\text{bern}}(\pi^*) \left(\frac{\partial \pi^*}{\partial x_d^*} \right)^2} = |\hat{\beta}_d| \sqrt{\pi^*(1 - \pi^*)}.$$

The R-sens importance measure for the logistic regression model is proportional to the absolute value of the regression coefficient. In addition, due to the logistic (inverse) link function, the local importance measure is higher for points close to the decision boundary $p(y^* = 1) = 0.5$ compared to points further away. Because the term $\sqrt{\pi^*(1 - \pi^*)}$ is the same for each predictor variable, ranking the variables with R-sens is equivalent to ranking with the absolute regression coefficients $|\hat{\beta}_d|$ in the limit of infinite data.

Contrary to the linear regression example in the main paper, in logistic regression, the R-sens measure gives more importance to observations further from the decision boundary. It can be interpreted in the sense that the derivative of the logistic prediction function, $\frac{\partial \pi^*}{\partial x_d^*} = \hat{\beta}_d \pi^* (1 - \pi^*)$ gives too much emphasis to points near the decision boundary, and the R-sens measure makes the sensitivity measure more even.

12.1.2 Inverse Normal Link Function

Now, the “success probability” parameter as a function of the predictor variables is the cumulative Normal distribution function

$$p(y^* = 1 | \mathbf{X}, \mathbf{y}, \mathbf{x}^*) := \pi^*(\mathbf{x}^*) = \Phi(\mathbf{x}^* \hat{\beta}).$$

The derivative of π^* with respect to x_d^* is

$$\frac{\partial \pi^*}{\partial x_d^*} = \hat{\beta}_d \mathcal{N}(\mathbf{x}^* \hat{\beta}).$$

The Fisher information of the Bernoulli distribution

$$\mathcal{I}_{\text{bern}}(\pi^*) = \frac{1}{\pi^*(1 - \pi^*)}.$$

In the limit when the number of observations goes to infinity, the R-sens measure thus evaluates to

$$\sqrt{\mathcal{I}_{\text{bern}}(\pi^*) \left(\frac{\partial \pi^*}{\partial x_d^*} \right)^2} = |\hat{\beta}_d| \frac{\mathcal{N}(\mathbf{x}^* \hat{\boldsymbol{\beta}})}{\sqrt{\pi^*(1-\pi^*)}}.$$

12.2 Poisson Regression Model

In a Poisson regression model, the predictive distribution is a Poisson distribution. Here, we consider the commonly used logarithmic link function, where the mean of the predictive distribution is

$$\mathbb{E}[y^*] = \exp(\mathbf{x}^* \boldsymbol{\beta}).$$

In the asymptotic limit of infinite data, the posterior of the regression coefficients concentrates to a point $\hat{\boldsymbol{\beta}}$, and the mean of the predictive distribution is given by the exponential function

$$\mathbb{E}[y^*] = \exp(\mathbf{x}^* \hat{\boldsymbol{\beta}}).$$

The derivative of $\mathbb{E}[y^*]$ with respect to x_d^* is

$$\frac{\partial \mathbb{E}[y^*]}{\partial x_d^*} = \hat{\beta}_d \exp(\mathbf{x}^* \hat{\boldsymbol{\beta}}).$$

The Fisher information of the Poisson distribution is

$$\frac{1}{\mathbb{E}[y^*]}.$$

In the limit when the number of observations goes to infinity, the R-sens measure thus evaluates to

$$|\hat{\beta}_d| \exp\left(\frac{1}{2} \mathbf{x}^* \hat{\boldsymbol{\beta}}\right).$$

The R-sens measure depends on \mathbf{x}^* , but the additional factor is the same for all predictors.